Department of Biomedical Sciences
University of Veterinary Medicine Vienna

Institute of Pharmacology and Toxicology
(Head: O.Univ.-Prof. Dr.med.vet. Mathias Müller)

Antileishmanial mechanism of sterol endoperoxides: Influence on ergosterol synthesis

Bachelor thesis submitted for the fulfilment of the requirements for the degree of

Bachelor of Science (BSc.)

University of Veterinary Medicine Vienna

submitted by

Elisabeth Maria Schrödl

Vienna, June 2023

The experiments for this thesis were conducted from February to May 2023 under the supervision of Ao. Univ.-Prof. Dr.rer.nat. Lars Gille at the Institute of Pharmacology and Toxicology in the Department of Biomedical Sciences.

Reviewer: Dipl.-Biol. Dr.rer.nat. Catharina Duvigneau
Institute for Medical Biochemistry
Department of Biomedical Sciences
University of Veterinary Medicine Vienna
Veterinärplatz 1
1210 Vienna

Acknowledgements

First of all, I would like to express my gratitude to Ao.Univ.-Prof. Dr.rer.nat. Lars Gille for providing me the great opportunity to write my bachelor thesis in his lab. I am deeply grateful for his unfaltering support, immense patience and encouraging advice throughout my work.

Additionally, I want to express my gratitude to Deblina Sarkar, Msc. for helping me with my practical work and throughout the process of writing my thesis. Furthermore, my sincere appreciation belongs to Ao.Univ.-Profin Drin rer.nat. Katrin Staniek and Sara Kapucu for creating a great work environment.
Moreover, I would like to thank Dipl.-Biol. Dr.rer.nat. Catharina Duvigneau for reviewing this thesis.

Lastly, I am grateful to my family and friends for their continuous support and encouragement throughout the process of working on my bachelor's thesis.

Table of Contents

1 Introduction 1
1.1 Sterols 1
1.2 Ergosterol synthesis as a drug target 2
1.3 Azoles target ergosterol biosynthesis pathway 3
1.4 Leishmania 4
1.4.1 Leishmania life cycle 4
1.4.2 Leishmaniasis 5
1.5 Current antileishmanial drugs 6
1.6 Endoperoxides 7
1.7 Sterol endoperoxides 7
1.7.1 Ergosterol endoperoxide 7
1.7.2 Dehydrocholesterol endoperoxide 8
1.8 Aims of the work 9
2 Materials and Methods 10
2.1 Chemicals 10
2.2 LtP cell culture 11
2.3 Influence of sterol EP on ergosterol content in LtP 11
2.3.1 Incubation of LtP with different concentrations of compounds 11
2.3.2 Ergosterol extraction 12
2.3.3 Determination of ergosterol in LtP 12
2.3.4 HPLC analysis of sterols in LtP 13
2.4 Viability assay 13
2.5 XO assay 15
2.5.1 Aerobic XO assay 15
2.5.2 Anaerobic XO assay 15
2.6 Inhibition on oxygen consumption of LtP 16
3 Results 17
3.1 Influence of sterol EP and related compounds on the viability of LtP 17
3.2 Reaction of sterol endoperoxides with Fe^{2+} 20
3.3 Influence of NAC on the antileishmanial activity of compounds 24
3.4 Inhibition on oxygen consumption of LtP 26
3.5 Influence of sterol EP on ergosterol content in LtP 28
4 Discussion 33
5 Summary 38
6 Zusammenfassung 39

7 Abbreviations 40
8 References.....41
9 List of Figures.....44
10 List of Tables 46

1 Introduction

1.1 Sterols

Sterols are substantial components of the membranes of eukaryotic organisms. They are crucial for vital functions, such as the control of membrane fluidity and permeability as well as for signaling functions.

There are three prevalent forms of sterols in eukaryotes: Cholesterol (Chol) in vertebrates, phytosterols (stigmasterol, sitosterol, campesterol) in plants and ergosterol (Ergo) in fungi and protozoa. Each of these sterols is the final product of a complex biosynthetic pathway branching from their common initial pathway from acetyl-CoA to squalene epoxide (Fig. 1) (1).

Squalene epoxide is converted to lanosterol, the precursor for biosynthesis of both Chol and Ergo (2).

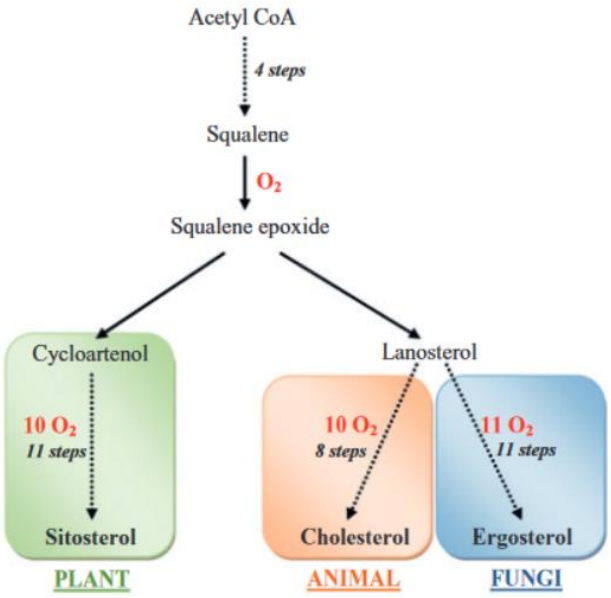

Figure 1: *Sterol biosynthesis pathways. Simplified biosynthesis pathway of sterols in plants, animals and fungi. All three share a common pathway to squalene epoxide. Subsequently, cycloartenol is formed in plants, and lanosterol in animals and fungi. The final products of the sterol pathways are sitosterol, cholesterol and ergosterol. The number of steps required in the metabolic pathways is shown in italics, and the number of oxygen molecules in red (1).*

Sterols form a group of organic compounds with a tetracyclic sterane backbone and a hydroxyl group at the 3-position of the A-ring. The chemical structure of Ergo varies from Chol due to the presence of a methyl group at C24 of the of the side chain and two additional double bonds at the positions C7 and C22 (Fig. 2) (3).

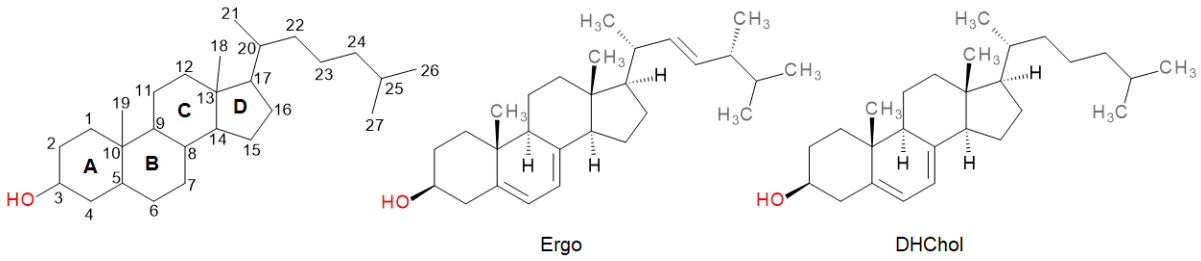

Figure 2: *Chemical structures of ergosterol (Ergo) and dehydrocholesterol (DHChol). The first structure illustrates the numbering of the C atoms and the four fused rings forming the tetracyclic sterane backbone. The sole difference between Chol and DHChol is the presence of a double bond between carbons 7 and 8 in DHChol. Their hydroxyl group is shown in red.*

Due to these structural differences, the respective sterols have some different functions and properties. For instance, Chol is less active as an antioxidant than Ergo (1). The antioxidant function of Ergo is related to the two conjugated double bonds of the B-ring and might be of particular importance for fungi and protozoa to combat oxidative stress. Free Ergo, which accumulates in the plasma membrane of fungal cells, may facilitate the protection of phospholipids from oxidative perturbation. In addition, the antioxidant function of Ergo may play a role in the still not entirely understood health benefits of consumption of some fungi (4).

Ergo is a precursor of vitamin D2 (ergocalciferol) in which it can be converted by ultraviolet light. This makes mushrooms a potent source of vitamin D, which contributes to their growing popularity as a nutritious food. Vitamin D, a fat-soluble, cyclopentane polyphenolic compound, is essential for the human body as it plays an important role in promoting calcium absorption and bone health. Furthermore, vitamin D deficiency has been linked to cancer, heart disease, neuropsychiatric disorders and other chronic diseases. The most abundant forms of vitamin D are vitamin D3, which is primarily produced by ultraviolet B (UVB) radiation in skin cells exposed to sunlight, and vitamin D2, which is mainly found in fungi and yeasts. Vitamin D2 and vitamin D3 are metabolized stepwise in both the liver and kidneys to 1,25$(OH)_2$D, which is the biologically active compound and thus useful form for the human body (5).

1.2 Ergosterol synthesis as a drug target

The Ergo biosynthetic pathway has been identified as a suitable drug target for both fungi and parasites as Ergo plays an essential role in modulating membrane dynamics, structure and mechanical properties but is not present in mammalian cells. Since the biosynthesis of Ergo involves a cascade of 25 different enzymes, it offers a variety of possible targets (6).

1.3 Azoles target ergosterol biosynthesis pathway

Azoles, five-membered heterocyclic compounds, are an important class of chemotherapeutic agents with a wide-spectrum of activity against filamentous fungi and yeasts. They are divided in two broad groups, which include imidazoles and triazoles. Imidazoles contain two nitrogens in the azole ring and include, for example, the antifungal/antiparasitic agents ketoconazole (KetoAz) and miconazole (MiAz). Triazoles contain three nitrogens in the azole ring and this group encompasses, for example, itraconazole (ItraAz) (Fig. 3) (6).

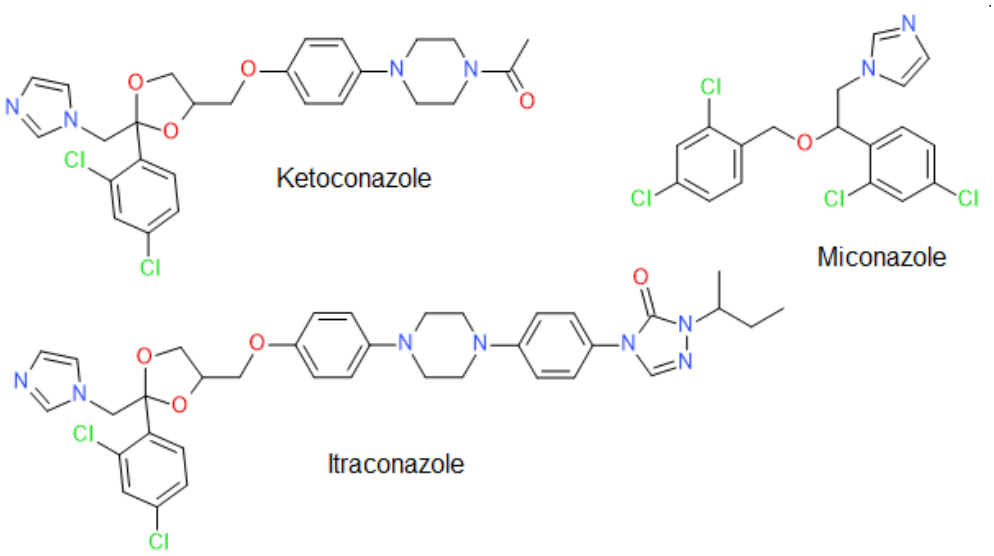

Figure 3: *Chemical structures of ketoconazole (KetoAz), miconazole (MiAz) and itraconazole (ItraAz). The two imidazoles, KetoAz and MiAz contain two nitrogens in the azole ring. ItraAz, is a triazole and contains three nitogens in the azole ring.*

Azoles are the most frequently used class of antifungal drugs for the treatment of *Candida* infections. *Candida* infections are among the most common fungal infections worldwide and mainly affect elderly, hospitalized or immunocompromised patients (6).

Azoles target the enzyme 14α-demethylase, an essential enzyme in Ergo biosynthesis. This enzyme demethylates lanosterol at the C14 position of the ring system, through three sequential oxidations and release of formic acid (2). When 14α-demethylase is inhibited, other enzymes in this pathway synthesize a fungistatically toxic sterol (14α methylergosta 8-24 (28) dienol). In addition, azoles are also increasing reactive oxygen species (ROS) levels in cells. Both the increased ROS levels and the production of toxic sterols lower the Ergo levels in the cell and, therefore, inhibit the growth of the infecting fungus (6).

In summary, azoles are being successfully used against a wide range of fungal infections, including, *Candida spp*., but also *Microsporum spp. Aspergillus fumigatus*, *Histoplasma capsulatum*, *Coccidioides immitis* and *Blastomyes dermatides*. Furthermore, azoles have been experimentally proven effective against *Trypanosoma cruzi*, and *Leishmania* (7).

1.4 Leishmania

1.4.1 Leishmania life cycle

Leishmania is a genus of obligate intracellular, protozoan parasites that are transmitted to humans and animals through the bite of infected female sandflies (8). Two developmental stages of *Leishmania* parasites can be distinguished: amastigotes and promastigotes (Fig. 4). In the promastigote stage, the parasites are flagellated, motile and located in the digestive tract of the sand fly. They multiply and progress through morphologically distinct stages of differentiation to become non-dividing, infectious metacyclic promastigotes and migrate into the sandfly's salivary gland. This enables them to be transferred to the mammalian host during blood feeding. The parasites get phagocytosed by macrophages in which they are present as the spherical, non-flagellated amastigotes. The intracellular amastigotes multiply and are released by lysis of the macrophages, which enables them to infect new host cells. By feeding blood from infected hosts, the sandfly ingests the parasites again and the life cycle of the *Leishmania* is completed (9).

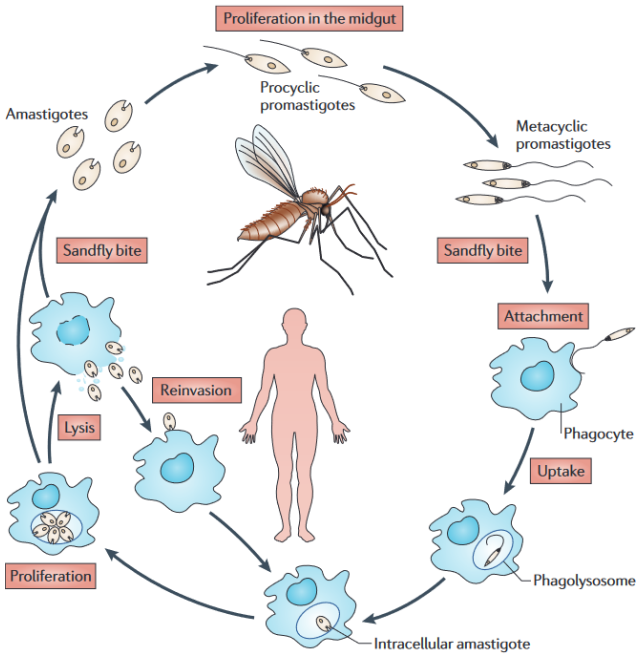

Figure 4: *The life cycle of Leishmania parasites. In sandflies, procyclic promastigotes differentiate into infectious, non-dividing metacyclic promastigotes, which are then transmitted to humans. The metacyclic promastigotes are phagocytosed by macrophages, intracellular amastigotes multiply and are released by macrophage lysis. The transmission cycle is completed when the infected phagocytes are ingested by another sandfly and the amastigotes are transform into promastigotes in the midgut of the sandfly (9).*

1.4.2 Leishmaniasis

These parasites cause a disease called leishmaniasis, that is present in over 90 countries, preferably in (sub)tropical regions. Most cases are recorded in Brazil, China, Ethiopia, India, Kenya, Somalia, Sudan and Nepal (8). Annually, between 700,000 and 1.2 million new cases of leishmaniasis are occuring, with an estimated 20,000 to 40,000 deaths every year. There are approximately 30 pathogenic species that can elicit diverse clinical manifestations. The most widespread species include *L. major, L. tropica, L. maxicana* and *L. infantum* (2). The form of the disease can also be influenced by other factors, such as the immune status of the host or malnutrition (8). The main phenotypic categories are cutaneous, visceral and mucosal leishmaniasis. Cutaneous leishmaniasis causes skin ulcers that may heal without treatment but can leave scars. Visceral leishmaniasis affects vital organs such as the spleen, liver and bone marrow and can lead to death if left untreated. Cutaneous leishmaniasis is mediated by a Th1 response, while visceral leishmaniasis is mediated by a Th2 response (9). Mucosal leishmaniasis affects the mucous tissue of the upper respiratory tract, extending from the inner nostril wall to the larynx and oral cavity. It can manifest several days to years after cutaneous leishmaniasis (10).

1.5 Current antileishmanial drugs

Antimonials have been used for 70 years as a primary treatment approach for visceral and cutaneous leishmaniasis, but their mechanism of action is still not thoroughly understood. Their use is limited by side effects and toxicity, as well as emerging resistance and therapeutic failures, especially in certain regions of the world. Upcoming resistances may be related to environmental factors, such as arsenic in drinking water in parts of India (11).

Amphotericin B is a polyene antibiotic, revealing its antileishmanial activity in the 1960s. It is obtained through fermentation of *Streptomyces nodosus* and is used to treat systemic fungal infections and as an antiprotozoal drug (11). The antibiotic primarily binds to Ergo of the *Leishmania* membranes, leading to the formation of channel structures and the release of cell components, especially potassium ions, and ultimately to cell death (12). Unfortunately, free amphotericin has a high toxicity and safer drug delivery systems like liposomal presentation are expensive and, therefore, not affordable for many regions and patients (11).

Miltefosine is a derivative of alkylphosphocholine. In addition to several species of *Leishmania*, miltefosin has also shown efficacy against a wide range of pathogenic fungi, various types of tumour cells, *Streptococcus pneumoniae* and diverse strains of *Acanthamoeba*. Miltefosin is an orally administered drug that has side effects such as gastrointestinal discomfort, loss of appetite, nausea, vomiting and diarrhoea due to its zwitterionic surfactant properties (13). The most significant disadvantage of this molecule is its long half-life (>120 h), which could favor the emergence of resistances (11).

Pentamidine enters the parasite via arginine and polyamine transporters, where it then accumulates and binds to the kinetoplast DNA. Due to pentamidine’s toxicity in visceral leishmaniasis treatment it is manly used against cutaneous leishmaniasis (11).

Currently, the control and therapy of leishmaniasis remains a severe problem due to several reasons: unavailability of a vaccine for humans, toxic side effects, high cost and the emergence of resistances for current chemotherapeutics (2). Therefore, the development of new antileishmanial agents with high potency, low cost, acceptable toxicity and pharmacokinetic properties is an urgent need.

1.6 Endoperoxides

Peroxides (RO-OR) are compounds characterized by two oxygen atoms connected by a single bond. Each oxygen atom is linked to another atom, usually hydrogen or carbon. An important subgroup are cyclic alkyl peroxides, known as endoperoxides (EPs). Their peroxide bridge has already been identified as an important pharmacophore in artemisinins responsible for antimalarial, antifungal, antiparasitic, antibacterial, cytotoxic and antitumor activities (14). Polycyclic endoperoxides naturally occur in plants, various species of marine invertebrates, algae, fungi, fungal endophytes and other microorganisms (15).

Many polycyclic EPs have shown antimalarial activity, irrespective of whether they are naturally or synthetically produced. One essential component of malaria treatment is the EP artemisinin, which is usually isolated from *Artemisia annua L.* plants. They are not solely effective against plasmodia, but also selectively toxic against obligate intracellular protozoan parasites of the genera *Toxoplasma*, *Leishmania* and *Coccidia* (15).

Other EPs, such as ascaridole, have also been effectively tested against *Leishmania* in vitro. Studies suggest that reductive cleavage of the EP bridge upon reaction with Fe^{2+} results in the formation of cytotoxic radicals, thus leading to cell damage (16).

1.7 Sterol endoperoxides

1.7.1 Ergosterol endoperoxide

Ergosterol endoperoxide (ErgoEP) is a polycyclic EP that occurs naturally in wild as well as cultivated fungi, algae, plants, lichens, anemones, corals and trees (Fig. 5) (17). ErgoEP, isolated from fungi, has been shown to have antitumor effects against prostate cancer, colon cancer, hepatocellular carcinoma, myeloma, and leukemia, as well as antioxidant, anti-inflammatory and antiviral properties, and can induce apoptosis of cancer cells. Furthermore, ErgoEP demonstrated antibacterial activity against *Escherichia coli* and *Staphylococcus aureus* (15). Although ErgoEP is widely available in natural sources, the most economical way to obtain it in large quantities is the photosensitized oxidation of Ergo (18).

ErgoEP has been successfully used against *Leishmania* in experimental models, but their influence on *Leishmania* viability and metabolism has not been studied in detail.

Studies have been conducted focusing on the antitrypanosomal function of ErgoEP, however they were related to *Trypanosoma cruzi.* In the course of these studies, it was found that the key protein that interacts molecularly with ErgoEP is sterol 14α-demethylase (CYP51). The oxygen/oxygen bound at the peroxide bridge allows an interaction with the heme iron in the active site of CYP51. This interaction could induce a burst of radicals acting as an enzymatic inhibitor generating carbonyl moieties or long lived radicals. The action of these radicals as enzyme inhibitors, or as generators of secondary free radicals and metabolite inactivators, could amplify their chemotherapeutic effect and apoptosis might be induced (17).

1.7.2 Dehydrocholesterol endoperoxide

7-Dehydrocholesterol (DHChol) is a biosynthetic precursor of Chol (Fig. 5). In mammals this intermediate exist only in minor amounts (19). As electrophilic diene, DHChol can react with various oxidants including singlet oxygen leading to the corresponding EP DHCholEP. DHCHolEP showed biological activity against several cancer cell lines with IC_{50} values in the low micromolar range (18).

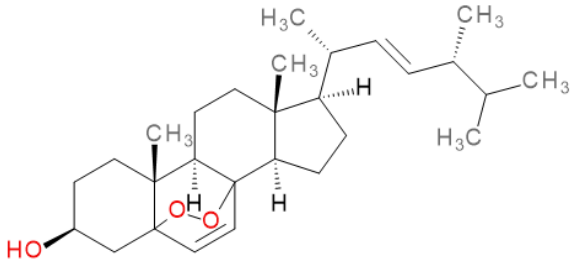

ErgoEP

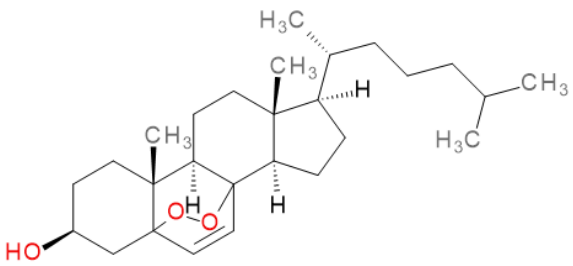

DHCholEP

Figure 5: *Chemical structures of ergosterol endoperoxide (ErgoEP) and dehydrocholesterol endoperoxide (DHCholEP). Their peroxide bridge and hydroxyl group are shown in red.*

1.8 Aims of the work

This bachelor thesis was focused on the antileishmanial activity and mechanism of the two synthetic sterol EPs: ErgoEP and DHCholEP.

The experiments of the thesis were performed to verify the following hypotheses:

(i) Sterol EPs inhibit LtP viability;
(ii) Their mechanism of action in LtP involves the formation of radicals by reaction with iron(II);
(iii) Their radical-mediated damage is prevented by the radical scavenger N-acetyl cysteine;
(iv) The enzymes of the Ergo synthesis pathway in *Leishmania* are most vulnerable due to the structure of sterol EPs which are similar to the enzymes' substrates;
(v) They cause mitochondrial inhibition.

2 Materials and Methods

2.1 Chemicals

The chemicals used for sample preparation and maintenance work in the course of this study are listed in Table 1.

Table 1: *List of chemicals used for maintenance work and sample preparation.*

Chemical	Supplier
Amphotericin B	Cayman Chemical
Antimycin A (AA)	Sigma-Aldrich (St. Louis, Missouri, USA)
Ascaridole (Asc)	Self- synthesized
Brain Heart Infusion medium (BHI)	Sigma-Aldrich (St. Louis, Missouri, USA)
Butylated hydroxytoluene (BHT)	Roche (Basel, Switzerland)
Cholesterol (Chol)	Sigma-Aldrich (St. Louis, Missouri, USA)
7-Dehydrocholesterol (DHChol)	Sigma-Aldrich (St. Louis, Missouri, USA)
Dehydrocholesterol endoperoxide (DHCholEP)	Self-synthesized
D(+)-glucose monohydrate	Merck (Darmstadt, Germany)
Dimethyl sulfoxide (DMSO)	VWR (Radnor, Pennsylvania, USA)
Ergosterol (Ergo)	Acros Organics (Geel, Belgium)
Ergosterol endoperoxide (ErgoEP)	Self-synthesized
Ethanol (EtOH)	Scharlab (Barcelona, Spain)
Hemin	Sigma-Aldrich (St. Louis, Missouri, USA)
H_2SO_4	Merck (Darmstadt, Germany)
Itraconazole (ItraAz)	Thermo Fisher Scientific (Waltham, MA, USA)
Ketoconazole (KetoAz)	Thermo Fisher Scientific (Waltham, MA, USA)
K_2HPO_4	Merck (Darmstadt, Germany)
KH_2PO_4	Merck (Darmstadt, Germany)
KOH	Merck (Darmstadt, Germany)
Methanol (MeOH)	Merck (Darmstadt, Germany)
Miconazole (MiAz)	Thermo Fisher Scientific (Waltham, MA, USA)
Miltefosine	Thermo Fisher Scientific (Waltham, MA, USA)
N-acetylcysteine (NAC)	Thermo Fisher Scientific (Waltham, MA, USA)

n-hexane	Merck (Darmstadt, Germany)
$(NH_4)_2Fe(SO_4)_2$	Sigma-Aldrich (St. Louis, Missouri, USA)
Penicillin-streptomycin solution	VWR (Radnor, Pennsylvania, USA)
Pentamidine (Pen)	Sigma-Aldrich (St. Louis, Missouri, USA)
Resazurin	Sigma-Aldrich (St. Louis, Missouri, USA)
Sodium dithionite	Sigma-Aldrich (St. Louis, Missouri, USA)
Xylenol orange (XO)	Sigma-Aldrich (St. Louis, Missouri, USA)
Yeast extract (YE)	Amresco (Solon, Ohio, USA)

2.2 LtP cell culture

For the experiments in this work the model system of *Leishmania tarentolae* promastigotes (LtP) (strain P10, Jena Bioscience, Germany) was employed. To cultivate LtP in 50 mL TubeSpin bioreactors, brain heart infusion (BHI) medium (37 g/L, pH 7.4) enriched with 5 mg/L hemin, 25000 IU/L penicillin and 25 mg/L streptomycin was used. The LtP were grown in an incubator (Cytoperm, Heraeus Instruments, Hanau, Germany) at 26.5 °C.

The cells were passaged three times a week, on Monday, Wednesday and Friday. To achieve the required cell count of about 36 * 10^6 LtP/mL on Mondays and Wednesdays and 18 * 10^6 LtP/mL on Fridays, the optical density at 600 nm was measured with a photometer (U-1100, Hitachi Ltd, Tokyo, Japan) and cell concentration was calculated using the following equation (20):

$$OD_{600} * 0.969 * 124 * 10^6 = \frac{LtP}{mL}$$

0.969: $converstion\ factor\ wet\left(\frac{g}{L}\right) - dry\ weight\ (g)$

124: $1\ g\ dry\ weight/L\ =\ 124 * 10^6\ LtP/mL$

2.3 Influence of sterol EP on ergosterol content in LtP

2.3.1 Incubation of LtP with different concentrations of compounds

As a first step, the total volume of BHI medium required for all concentrations was added to a sterile beaker. The BHI medium was then enriched with an aliquot of the current running cell culture to achieve a target optical density of 0.15. After mixing, 15 mL each of the cell suspension were transferred to 50 mL blue cap Falcon tubes and the respective concentration

of compound was added. For each concentration a duplicate sample was made. Ethanol was used as a vehicle control. Two air holes were drilled in the lids of each tube, to ensure that the LtP were supplied with a sufficient amount of oxygen during the incubation period. The incubation time was 28 or 48 hours depending on the compound. During this time period, the cell density was determined photometrically after 0, 5, 24 and optionally 48 hours. The final cells density prior to extraction was used to calculate the percentage of growth for the tubes of compounds with respect to tubes without compounds (100%).

2.3.2 Ergosterol extraction

In preparation for the extraction, empty 5 mL MCT tubes were weighed. The LtP culture was spun down in 50 mL tubes (3000 x g, 10 min, 20 °C). Next, the supernatant was discarded and the remaining pellet was resuspended in 5 mL PBS and transferred into the 5 mL MCT tubes. After centrifugation (4000 x g, 10 min, 20 °C) and discarding the supernatant, the tubes containing the pellets were weighed. 25 mL saponification solution (6.25 g KOH, 8.75 mL H_2O in ethanol) were prepared and 1.5 mL were added to each MCT tube. Subsequently, the tubes were incubated for 1 h at 85 °C and vortexed every 15 minutes. After the tubes cooled down to room temperature, 0.5 mL H_2O and 1.5 mL n-hexane were added to each tube. The transparent organic phase (1.2 mL) was extracted from each tube after vortexing (800 rpm, 30 min, 20 °C) on an Eppendorf thermomixer and centrifugation (4000 xg, 10 min, 20 °C) and transferred to an empty 1.5 mL Eppendorf tube.

2.3.3 Determination of ergosterol in LtP

To photometrically determine the wet weight (%) of ergosterol equivalents of each cell pellet, 200 µL of the respective extracted organic phase were solved in 1 mL ethanol in a quartz glass cuvette (Hellma, Müllheim, Germany). A spectrum in the range of 220 nm – 360 nm was recorded using a U-3300 UV-VIS spectrophotometer (HITACHI**,** Japan). Ethanol was used as a reference. The mass of ergosterol (mg) was calculated according to the following equation:

$$m_{ergo} = \frac{A_{282\,nm}}{\varepsilon_{282\,nm} * 0.001 * M_{ergo} * 1000 * F_{dilution}}$$

$A_{282\,nm} = absorption\ at\ 282\,nm$

$\varepsilon_{282\,nm} = 12150\ M^{-1}cm^{-1}$

$M_{ergo} = 396.65\ \frac{g}{mol}$

$F_{dilution} = 6$

After calculation of the ergosterol mass, the ergosterol equivalents' wet weight (%) was obtained by the equation:

$$ergosterol\ equivalents'\ wet\ weight\ (\%) = \frac{m_{ergo}}{m_{pellet}} * 100$$

2.3.4 HPLC analysis of sterols in LtP

Hexane extracts of weighed LtP pellets after saponification, liquid-liquid extraction with 1.5 ml hexane and photometric determination of Ergo-like molecules, were evaporated to dryness overnight. Dried extracts were dissolved in ACN with the volume equivalent to the hexane volume remaining after photometry and filled into HPLC sample vials.
HPLC analysis was performed on a Shimadzu LC-20 system including a dual-wavelength UV detector. With the integrated autosampler 10 µL of each sample were injected on a RP-8 column (LiChrospher®, analytical grade RP-8, particle size 5 µm, ID 4 mm, length 250 mm) with a pre-column (LiChrospher®, RP-8, particle size 5 µm, ID 4 mm, length 4 mm) and eluted with a mixture of 10 % H_2O and 90 % of a solvent mixture ACN/MeOH (99/1) for 30 min. Peaks were detected in the UV range at 205 nm and 281 nm and their area was measured for quantitation. Samples of pure substance were detected: DHCholEP, 6.9 min; ErgoEP, 7.1 min; DHChol, 14.3 min; Ergo, 14.4 min and Chol, 18.5 min. A major peak in LtP extracts was detected at 12.2 min showing strong absortion both at 281 and 205 nm. Spectra of the individual peaks were obtained by stopping the HPLC flow at the time of the expected peak maximum and initiating a spectral scan by the UV detector.

2.4 Viability assay

To conduct the viability assays 96-well non-treated cell culture plates were used (Eppendorf, Germany, Art. nr. 30730011). First, the assay medium was prepared, consisting of YEM medium (20.7 g/L yeast extract powder, 1.2 g/L K_2HPO_4, 0.2 g/L KH_2PO_4, 2.9 g/L glucose) mixed in a 1:1 ratio with PBS and supplemented with 25000 IU/L penicillin, 25 mg/L streptomycin and 6 µM hemin. A cell suspension containing $2*10^6$ LtP/mL was prepared using a fraction of the assay medium.

Two different viability assays were carried out, one with a vertical and one with a horizontal dilution series. Using the vertical viability assay, four different substances, each as a triplicate, were tested in six different concentrations. In the horizontal viability assay only three compounds, each as a duplicate, were tested but in twelve different concentrations.

For the horizontal viability assay the wells only containing medium (row A, column 1- 6; row H, column 7-12) were filled with 200 µL assay medium, whereas the test wells (row B-G, column 1-12) and the control wells with cells (row A, column 7-12; row H, column 1-6) were filled with 100 µL assay medium. In column 1, additional assay medium and aliquots of the compound stocks were added according to the designated compound concentrations. A 1:2 serial dilution was performed for all columns from row B to row G and 100 µL of cell suspension were added to all test wells. After placing 8 mL PBS between wells for humidity control the plate was incubated for 48 h at 26.5 °C.

For the vertical assay, the cell suspension was split into two equal parts, one of which remained unchanged as a control cell suspension and the second one was spiked with 2 mM N-acetylcysteine (NAC). In the control wells (row A) 200 µL assay medium were distributed.

To test the influence of NAC on the cell viability the columns 1-6 (Row B-G) were filled with the control cell suspension and the columns 7-12 were filled with the NAC cell suspension. In row H, additional control cell suspension (column 1-6), NAC cell suspension (column 7-12) were added and mixed with aliquots of the compound stocks according to the designated compound concentrations. Then a 1:2 serial dilution was performed from row H to row C and 8 mL PBS were added between the wells, the plate was incubated for 48 h at 26.5 °C.

After incubation, 50 µL resazurin (final concentration 20 µM) were added to each well followed by a second incubation period of 4 h under the same conditions. The fluorescence was measured at 590 nm emission with 560 nm excitation using a plate reader (Varioskan, Thermo Fisher Scientific, Waltham, USA). The viability (%) was calculated according to the formula from Fluorescence values of the wells with medium only (F_{Well_Medium}), wells with cells only ($F_{WellCell\_only}$) and wells with cells and respective compounds (F_{Well_Comp}).

$$Viability\ (\%) = \frac{F_{Well\_Comp} - F_{Well\_Medium}}{(F_{Well_{Cell\_only}} - F_{Well_{Medium}})}$$

To calculate the IC_{50} values a customized excel worksheet with python implementations was used.

2.5 XO assay

2.5.1 Aerobic XO assay

To conduct the XO assays, an organic peroxide reagent (0.125 mM xylenol orange, 4 mM butylated hydroxytoluene, 90 % methanol) was prepared. Immediately before starting the experiments the organic peroxide reagent was mixed with a freshly prepared iron stock (25 mM $(NH_4)_2Fe(SO_4)_2$, 2.5 M H_2SO_4) in the ratio of 1:100, resulting in a final concentration of 250 µM Fe^{2+}. Methanol was used as a reference. 1000 µL organic peroxide reagent mixed with iron stock were placed in an 1.5 mL disposable cuvette (BRAND, Wertheim, Germany) and 5 µL of the respective compound stock (20 mM) were added (100 µM final concentration). The optical density was measured for 20 minutes, in 20 second intervals in the range of 400 nm – 700 nm using a MS1501 UV-VIS diode array spectrophotometer (Shimadzu, Japan). For the kinetic evaluation the absorption at a wavelength of 560 nm was used. The slope of the xylenol/Fe^{3+} complex formation due to the reaction of the compound stocks with Fe^{2+}, was converted to the concentration change (nmol/min) via the extinction coefficient of the XO/Fe^{3+} complex (15000 L * mol^{-1} * cm^{-1}).

2.5.2 Anaerobic XO assay

Two 15 mL falcon tubes, tube A and tube B, were prepared for the anaerobic assay. In tube A, organic peroxide reagent and iron stock were mixed in the ratio of 1:50. In tube B, organic peroxide reagent was mixed with the respective compound (200 µM). Next, both tubes were flushed with nitrogen for 20 minutes. To perform the anaerobic XO assays, QS cuvettes (Hellma, Müllheim, Germany) with a PTFE stopper were used and the reagents were stirred by a magnetic stirrer for the duration of the experiment. Using a syringe rinsed with nitrogen, 750 µL solution were aspirated from tube B and dispensed into the cuvette, which had also been previously flushed with nitrogen. The cuvette was placed into the photometer and after the first measurement was taken, 750 µL from Tube A were added. During the measurements the cuvette was hermetically sealed with a stopper. The XO / Fe^{3+} formation rates were calculated analogously to the aerobic experiments.

2.6 Inhibition on oxygen consumption of LtP

To measure the oxygen concentration and consumption, Oxoplates with a round bottom (type OP96U) (PreSens Precision Sensing, Regensburg, Germany) with integrated chemical optical oxygen sensors were used. The oxygen sensors are composed of an indicator and reference layer. The fluorescence was measured at 540 nm excitation and 650 nm emission for the indicator layer and at 540 nm excitation and 590 nm emission for the reference dye (Varioskan, Thermo Fisher Scientific, Waltham, USA).

Prior to kinetic measurements the Oxoplate was calibrated, performing a two-point calibration with air-saturated BHI-medium and oxygen-free BHI-medium. The BHI-medium was air-saturated by agitating with a magnetic stirrer in an open baker for half an hour and deoxygenated by adding sodium dithionite (50 mg/mL).

For determining the inhibition of oxygen consumption of LtP (% of control) upon addition of different concentrations of mitochondrial inhibitors and test compounds, the test wells were first prepared. 50 µL air-saturated BHI-medium was added to the rows B-H. Additional air-saturated BHI-medium and aliquots of the compound stocks were added according to the designated compound concentrations in row C. Then a 1:2 serial dilution was performed from row C to row H. A cell suspension consisting of 140 * 10^6 LtP/mL was prepared in additional air-saturated BHI-medium and 150 µL were added into each well from row B and H immediately before the measurement. Lastly, 80 µL paraffin oil was added on top of each well. Then the sealed Oxoplate was inserted into the plate reader and oxygen concentrations were monitored for 39 min in 3 min intervals. Oxygen consumption values were calculated in a customized Excel worksheet.

3 Results

3.1 Influence of sterol EP and related compounds on the viability of LtP

An important pharmacological parameter for potential new anti-leishmanial compounds is the concentration at which these compounds eliminate half of the *Leishmania* cells after incubation, the IC_{50}. In this study the compounds were tested in different concentration ranges according to their activity regarding the influence on the viability of LtP after 48 hours of incubation using resazurin as indicator dye. The following graphs show typical examples of viability-concentration curves.

The comparison of ErgoEP and Ergo shows that both compounds are active against LtP, while the EP has a lower IC_{50} value than the parent sterol (Fig. 6). Both compounds show a rather steep decrease of the viability-concentration curve.

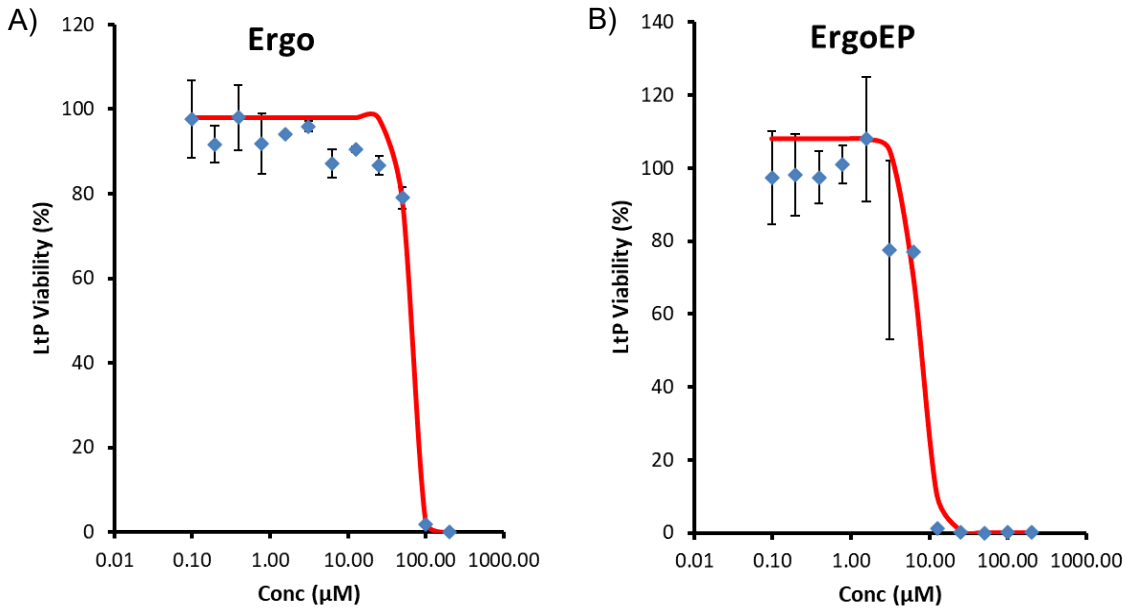

Figure 6: *Typical example of LtP viability (%) influenced by different concentrations (0.098 µM – 200 µM) of A) ergosterol (Ergo) or B) ergosterol peroxide (ErgoEP). Viability-concentration curves were determined using a horizontal viability assay, and each data point was calculated by taking the mean ± standard deviation of two replicates. The resulting IC_{50} values are A) 60.775 µM ± 3.63 µM, B) 7.26 µM ± 1 µM.*

Furthermore, DHCholEP and DHChol are both active against LtP. Again, the EP has a lower IC_{50} value than the parent sterol (Fig. 7). Both compounds show a rather steep decrease of the viability-concentration curve.

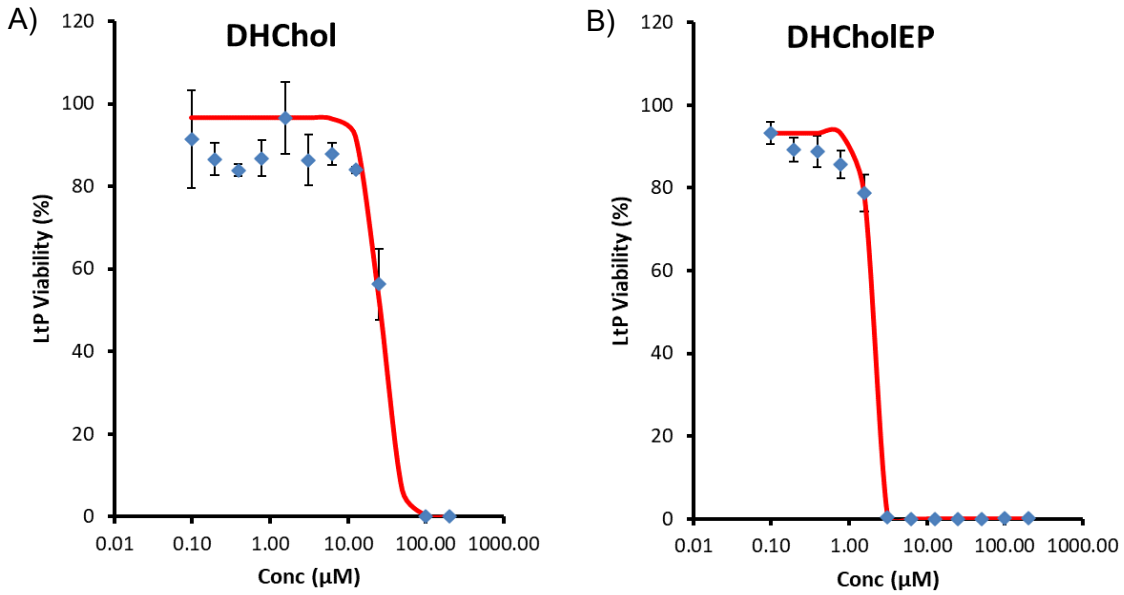

Figure 7: *Typical example of LtP viability (%) influenced by different concentrations (0.098 µM – 200 µM) of A) dehydrocholesterol (DHChol) or B) dehydrocholesterol endoperoxide (DHCholEP). Viability-concentration curves were determined using a horizontal viability assay, and each data point was calculated by taking the mean ± standard deviation of two replicates. The resulting IC_{50} values are A) 26.25 µM ± 1.59 µM, B) 1.87 µM ± 0 µM.*

In addition, typical anti-leishmanial agents, such as miltefosine and amphotericin B were included in the study. While miltefosine demonstrated an IC_{50} value in the low micromolar range, amphotericin B was already active at nanomolar concentrations (Fig. 8).

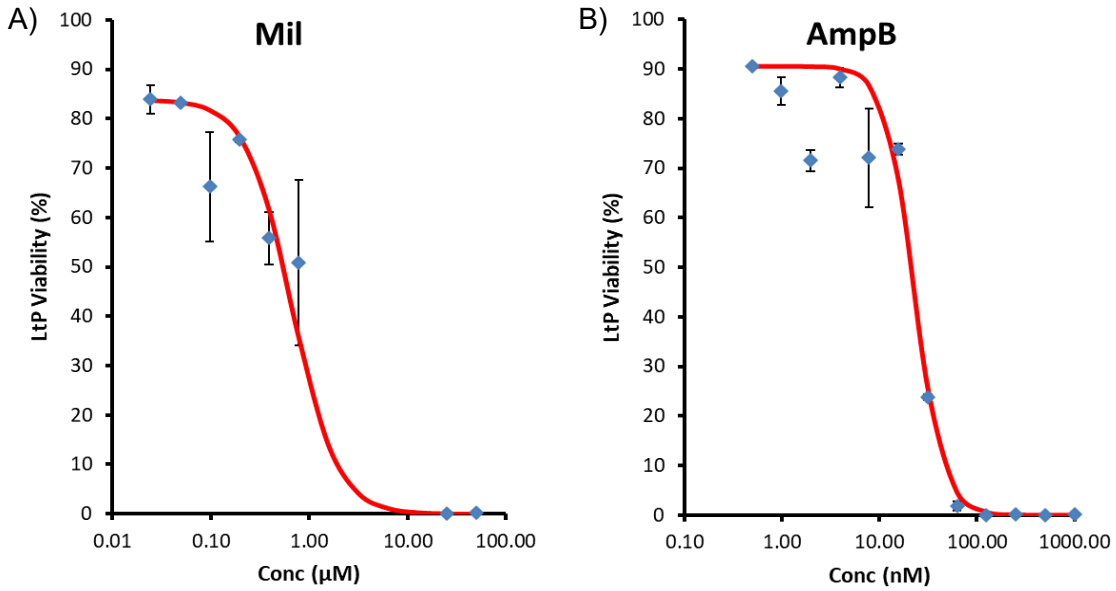

Figure 8: *Typical example of LtP viability (%) influenced by different concentrations of A) miltefosine (Mil) (0.024 µM - 50 µM) or B) Amphotericin B (AmpB) (0.488 nM – 1000 nM). Viability-concentration curves were determined using horizontal viability assay, and each data point was calculated by taking the mean ± standard deviation of two replicates. The resulting IC_{50} values are A) 0.67 µM ± 0.47 µM, B) 22.69 nM ± 2 nM.*

Since the current study also aimed at elucidating the anti-leishmanial mechanism of sterol EPs, also antifungal compounds, known to inhibit Ergo synthesis in yeast, were included. The three selected compounds were active in the nanomolar and micromolar inflation range. Surprisingly, the viability-concentration curves for KetoAz and IntraAz are rather shallow compared to MiAz and other studied compounds (Fig. 9).

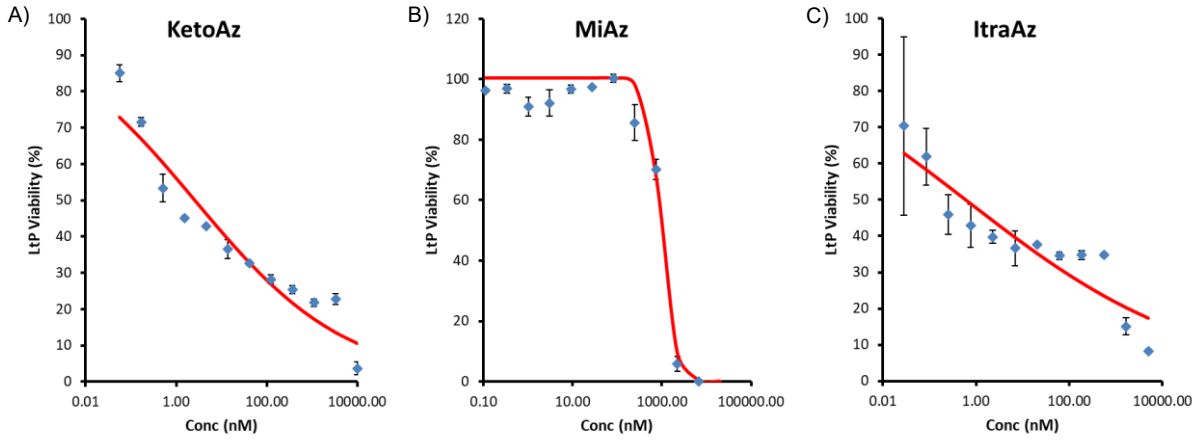

Figure 9: *Typical example of LtP viability (%) depending on different concentrations of A) ketoconazole (KetoAz, 0.056 nM – 10000 nM), B) miconazole (MiAz, 0.113 nM – 20000 nM) or C) itraconazole (IntraAz, 0.028 nM – 5000 nM). Viability-concentration curves were determined using a horizontal viability assay, and each data point was calculated by taking the mean ± standard deviation of two replicates. The resulting IC50 values are A) 2.588 nM ± 1.037 nM, B) 965.79 nM ± 97 nM, and C) 0.596 nM ± 0.027 nM.*

These typical examples of viability-concentration curves represent results from single culture dates. To reflect the biological variability of a cell culture over time, these experiments were repeatedly performed over 4 - 5 weeks and the resulting individual IC_{50} values were averaged and displayed in table 2.

***Table 2**: Influence of the respective compound on the viability of LtP. Mean IC_{50} value ± standard deviation of the respective compounds of 4-6 replicates performed over 4 - 5 weeks. The data were obtained by horizontal viability assays, with the concentrations of compounds used ranging from 0.010 µM – 20 µM for pentamidin (Pen), from 0.098 µM – 200 µM for cholesterol (Chol), ergosterol (Ergo), ergosterol endoperoxide (ErgoEP), dehydrocholesterol (DHChol) and dehydrocholesterol endoperoxide (DHCholEP), from 0.056 nM – 100000 nM for ketoconazole (KetoAz), from 0.028 nM – 20000 nM for itraconazole (IntraAz), from 0.113 nM – 20000 nM for miconazole (MiAz), from 0.024 µM – 50 µM for miltefosine (Mil) and from 0.488 nM – 1000 nM for amphotericin B (AmpB).*

Compound	IC_{50} (µM) Mean ± SD
Pen	0.625 ± 0.253
Chol	>200
Ergo	32.486 ± 16.870
ErgoEP	7.645 ± 1.995
DHChol	13.401 ± 9.585
DHCholEP	2.253 ± 0.690
Mil	0.446 ± 0.137
AmpB	0.019 ± 0.009
KetoAZ	0.003 ± 0.004
ItraAZ	0.004 ± 0.006
MiAZ	0.641 ± 0.403

The comparison of averaged IC_{50} values reveals that depending on the compound class a different anti-leishmanial activity is observed. While the sterol Chol is inactive, the sterols Ergo and DHChol show a significant anti-leishmanial activity and the corresponding EPs are even more active. The reference compounds with different targets in *Leishmania* all show a high activity in the low micromolar or millimolar range.

3.2 Reaction of sterol endoperoxides with Fe^{2+}

The reaction of Fe^{2+} with EPs and reference compounds was studied in a xylenol orange assay. In an initial experiment the reaction of the compound vehicle ethanol (EtOH), the sterol Chol and the terpenic EP ascaridole (Asc) was studied (Fig. 10). After addition of aliquots of the compound stocks, no formation of the XO/Fe^{3+} complex was observed for Chol and EtOH. In contrast, upon addition of Asc a linear increase of the absorption of this complex was observed.

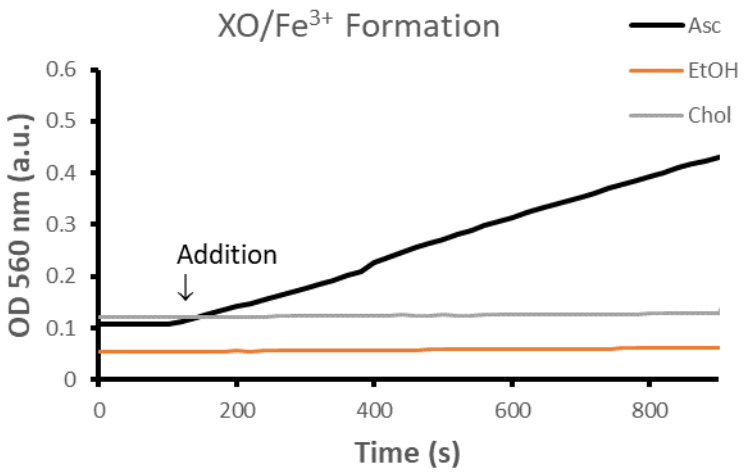

Figure 10: *XO/Fe^{3+} complex formation due to the reaction of ascaridole (Asc, 100 µM), ethanol (EtOH, 5 µL) or cholesterol (Chol, 100 µM) with Fe^{2+} (250 µM), dissolved in 1000 µL organic peroxide reagent. The complex formation was measured at a wavelength of 560 nm, every 20 seconds, for a total of 20 minutes. The experiment was performed in disposable cuvettes, without stirring and in the presence of air. Time traces represent typical examples of triplicate measurements.*

The reaction of ErgoEP with Fe^{2+} was studied in comparison to the reaction of the parent compound Ergo (Fig. 11). After addition of the compound aliquots a non-linear increase of the complex absorption was observed.

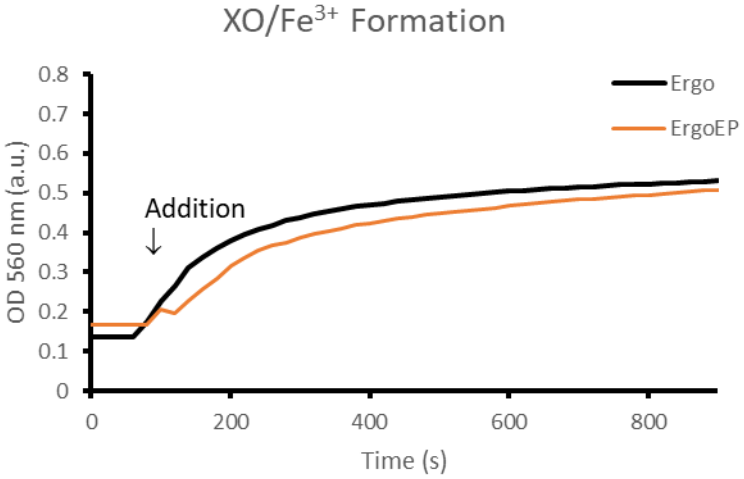

Figure 11: *XO/Fe^{3+} complex formation due to the reaction of ergosterol (Ergo, 100 µM) or ergosterol endoperoxide (ErgoEP, 100 µM) with Fe^{2+} (250 µM), dissolved in 1000 µL organic peroxide reagent. The complex formation was measured at a wavelength of 560 nm, every 20 seconds, for a total of 20 minutes. The experiment was performed in disposable cuvettes, without stirring and in in the presence of air. Time traces represent typical examples of triplicate measurements.*

Likewise, the reaction of DHCholEP with Fe^{2+} was studied in comparison to the reaction of the parent compound DHChol (Fig. 12). Also in this case, after addition of the compound aliquots a nonlinear increase of the complex absorption was observed.

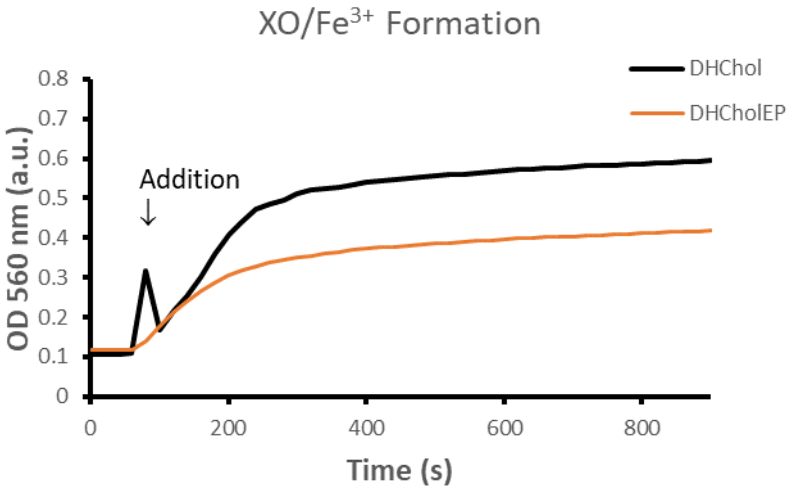

Figure 12: *XO/Fe^{3+} complex formation due to the reaction of dehydrocholesterol (DHChol, 100 µM) or dehydrocholesterol endoperoxide (DHCholEP, 100 µM) with Fe^{2+} (250 µM), dissolved in 1000 µL organic peroxide reagent. The complex formation was measured at a wavelength of 560 nm, every 20 seconds, for a total of 20 minutes. The experiment was performed in disposable cuvettes, without stirring and in the presence of air. Time traces represent typical examples of triplicate measurements.*

For a kinetic evaluation of the xylenol/Fe^{3+} complex formation, the initial slopes of the absorption increases were measured, and the formation rates were calculated (Tab. 3).

Table 3: *Mean XO / Fe^{3+} formation rates (nmol/min) ± standard deviation of three measurements with the respective compounds. The XO/Fe^{3+} complex formation results from the reaction of the respective compound (100 µM) with Fe^{2+} (250 µM), dissolved in 1000 µL organic peroxide reagent. The complex formation was measured at a wavelength of 560 nm, every 20 seconds, for a total of 20 minutes. The experiment was performed in disposable cuvettes, without stirring and in the presence of air.*

Compound	**XO / Fe^{3+} formation rate (nmol/min) Mean ± SD**
EtOH	0.03 ± 0.00
Asc	1.49 ± 0.18
Chol	0.03 ± 0.01
Ergo	9.61 ± 1.38
ErgoEP	7.24 ± 0.19
DHChol	14.00 ± 0.40
DHCholEP	8.55 ± 0.97

The rate of the EP Asc was higher than the rates of the control compounds EtOH and Chol. The rates of the sterol EPs were even higher than the rates of Asc. Unexpectedly, the sterol parent compounds displayed even faster rates than the corresponding sterol EPs. Since this could indicate peroxidation reaction of the sterols supported by oxygen, the influence of the presence and absence of oxygen on these rates was studied in further experiments (Tab. 4).

Table 4: *Mean XO / Fe^{3+} formation rates (nmol/min) ± standard deviation of three measurements with the respective compounds and conditions. The XO/Fe^{3+} complex formation results from the reaction of ergosterol (Ergo, 100 µM), or dehydrocholesterol (DHChol, 100 µM) with Fe^{2+} (250 µM), dissolved in 1000 µL organic peroxide reagent. The complex formation was measured at a wavelength of 560 nm, every 20 seconds, for a total of 20 minutes. The data were obtained by experiments either with stirring and flushing the compounds with nitrogen for 20 minutes or without stirring and in the presence of air.*

Compound + Condititon	**XO / Fe^{3+} formation rate (nmol/min) Mean ± SD**
Ergo + Air	7.91 ± 1.71
Ergo + N_2	11.76 ± 2.21
DHChol + Air	6.18 ± 1.67
DHChol + N_2	10.74 ± 1.21

Surprisingly, in these experiments the attempt to remove oxygen from the reaction system (+ N_2) did not decrease the reaction rates of sterols in the xylenol orange assay. In contrary, the reaction rates were slightly higher in the experiments with N_2 treatment than in the presence of air.

To further evaluate the role of oxygen in the reaction of sterols with Fe^{2+}, the reaction of sterols in a water/ethanol mixture were studied in Oxoplates to determine oxygen consumption. Air saturated solvent mixtures with the corresponding sterol were admixed with aliquots of Fe^{2+}. Four minutes after mixing the oxygen concentrations were measured in 3 - minute intervals. The results demonstrated that the reaction (if there was any) occurred already in the first 4 minutes after mixing. The oxygen concentrations after mixing were summarized in Table 5. As can be seen, Fe^{2+} alone already consumed significant amounts of oxygen in this time. In the presence of additional Ergo this is not further increased, however, in the presence of DHChol even more oxygen was consumed.

Table 5: *Mean oxygen concentration (µM) ± standard deviation of three measurements. The data were obtained by experiments with Fe^{2+} (625 µM), or Fe^{2+} (625 µM) mixed with ether ergosterol (Ergo, 100µM) or dehydrocholesterol (DHChol, 100µM), solved in 80 % H_2O / 20 % Methanol. PBS was used for control.*

Compounds	Oxygen Conc (µM) Mean ± SD
Control	275 ± 5
Fe(II)	231 ± 2
Ergo + Fe(II)	230 ± 11
DHChol + Fe(II)	151 ± 10

3.3 Influence of NAC on the antileishmanial activity of compounds

The anti-leishmanial mechanism of compounds can depend on various different mechanisms. If the anti-leishmanial activity of a compound includes extensive formation of reactive oxygen species (ROS) the activity should be strongly influenced by the availability of antioxidants in *Leishmania*. N-acetyl cysteine (NAC) is a potent thiol antioxidant and radical scavenger. In the presence of this compound the IC_{50} values of anti-leishmanial drugs should be increased if their mechanism is based on extensive ROS formation. Therefore, corresponding experiments were performed with sterol EPs, sterols and reference compounds.

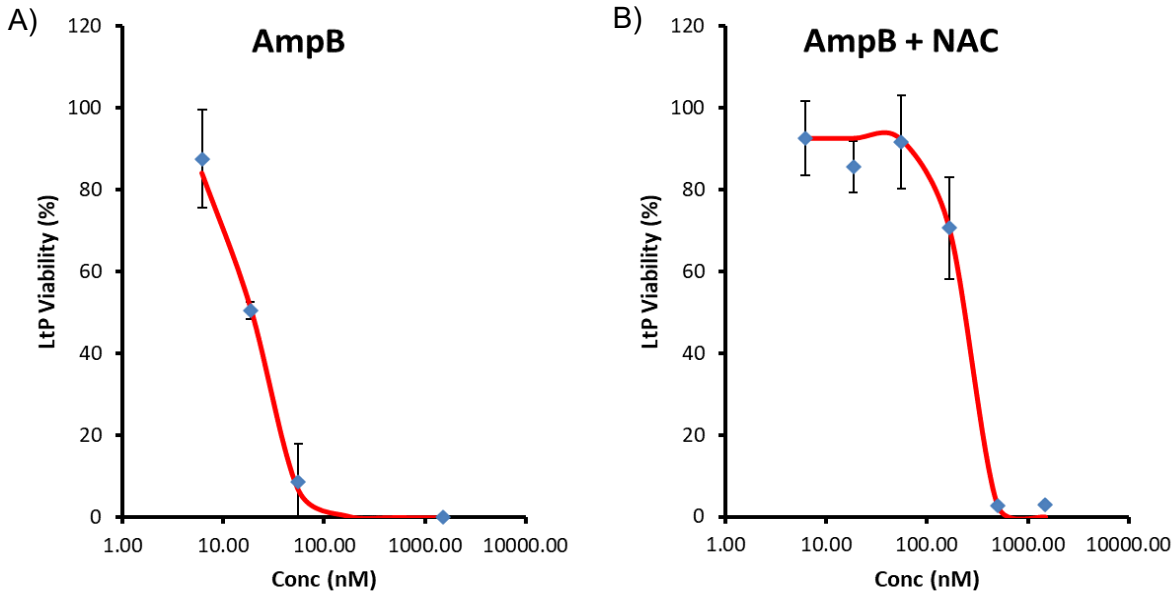

Figure 13: *A) Typical example of LtP viability (%) depending on different concentrations (6.17 nM – 1500 nM) of amphotericin B (AmpB). The influence of N-acetyl cysteine (NAC, 2 mM) on the IC_{50} value is illustrated in diagram B). Viability-concentration curves were determined using a vertical viability assay, and each data point was calculated by taking the mean ± standard deviation of three replicates. The resulting IC_{50} values are A) 21.31 nM ±, 0.26 nM, B) 220.26 nM ± 20.20 nM. The resulting change of the IC_{50} value in this case was calculated to be 1033.45 %.*

A typical example of viability-concentration curves for AmpB in the absence and presence of NAC is shown in figure 13. This example demonstrates that in the presence of NAC AmpB has at least 10 times less anti-leishmanial activity, in comparison to AmpB alone.
Furthermore, analogous experiments were performed for other compounds in this study and the averaged changes of IC_{50} values for the individual compounds are summarized in table 6.

Table 6: *Relative change of mean IC_{50} values (%) ± standard deviation of four replicates upon addition of N-acetyl cysteine (NAC, 2mM). The data were obtained by vertical viability assays, with the concentrations of compounds used ranging from 0.082 µM – 200 µM for ergosterol (Ergo), ergosterol endoperoxide (ErgoEP), dehydrocholesterol (DHChol) and dehydrocholesterol endoperoxide (DHCholEP), from 0.643 nM – 20000 nM for itraconazole (IntraAz), from 2.572 nM – 20000 nM for miconazole (MiAz), from 0.010 µM – 40 µM for miltefosine (Mil) and from 0.190 nM – 1500 nM for amphotericin B (AmpB).*

Compound	Relative change of IC_{50} (%) Mean ± SD
Ergo	139 ± 46
ErgoEP	148 ± 59
DHChol	153 ± 28
DHCholEP	137 ± 69
Mil	86 ± 27
AmpB	736 ± 288
ItraAZ	96 ± 39
MiAZ	101 ± 71

In this assay, sterols and sterol EPs show values above 100 %, however most of them have a high standard deviation. This indicates that the influence of the hydrophilic radical scavenger NAC on the anti-leishmanial activity of these compounds is small or marginal. NAC demonstrated a strong effect on AmpB activity, clearly indicating the involvement of ROS in its mechanism. Other compounds including antifungal azoles did not show an influence of NAC on the IC_{50} values.

3.4 Inhibition on oxygen consumption of LtP

Mitochondria are essential for the survival of LtP. A major function of these organelles is oxidative phosphorylation using the electron transfer chain consuming oxygen for generation of a proton gradient which in turn is used for ATP synthesis. To assess the direct effect of drugs on the mitochondrial electron transfer chain in LtP the oxygen consumption of LtP in the presence of compounds was measured.

In figure 14, the influence of antimycin A (AA), a mitochondrial inhibitor, and pentamidine targeting non-mitochondrial functions, on LtP oxygen consumption is shown. While AA demonstrates a clear dose-dependent inhibition of oxygen consumption in LtP, pentamidine had only marginal effects on this metabolic function.

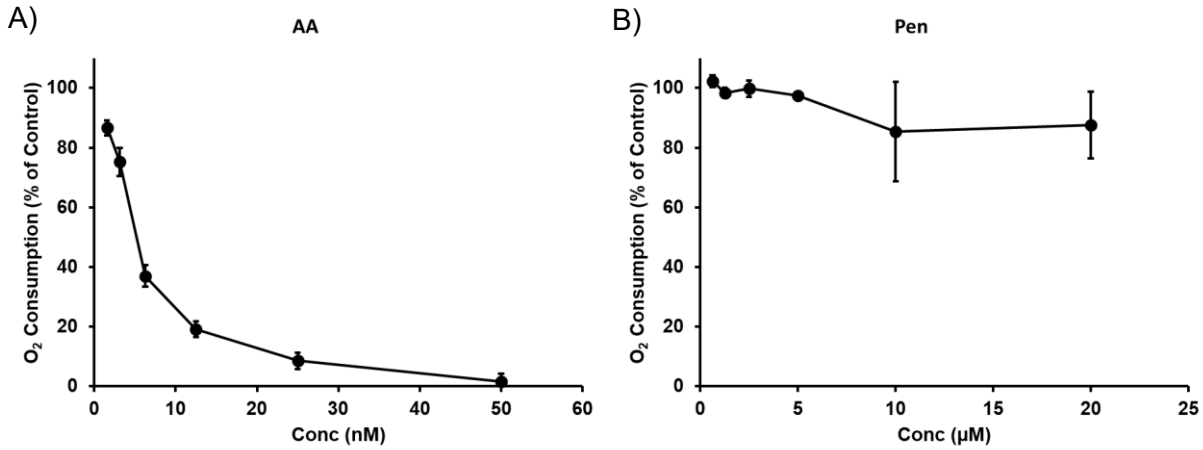

Figure 14: *Inhibition of oxygen consumption of LtP (% of control) depending on different concentrations of A) antimycin A (AA, 1.56 nM – 50 nM) or B) pentamidine (Pen, 0.63 µM – 20 µM). The oxygen consumption was measured for a total of 40 minutes. The experiments were conducted in air-saturated BHI medium mixed with 140 Mio/mL LtP. Data points represent mean ± standard deviation of 4 wells.*

For Ergo and ErgoEP only small effects on mitochondrial oxygen consumption of LtP were observed at concentrations much higher than their IC_{50} value in LtP (Fig. 15).

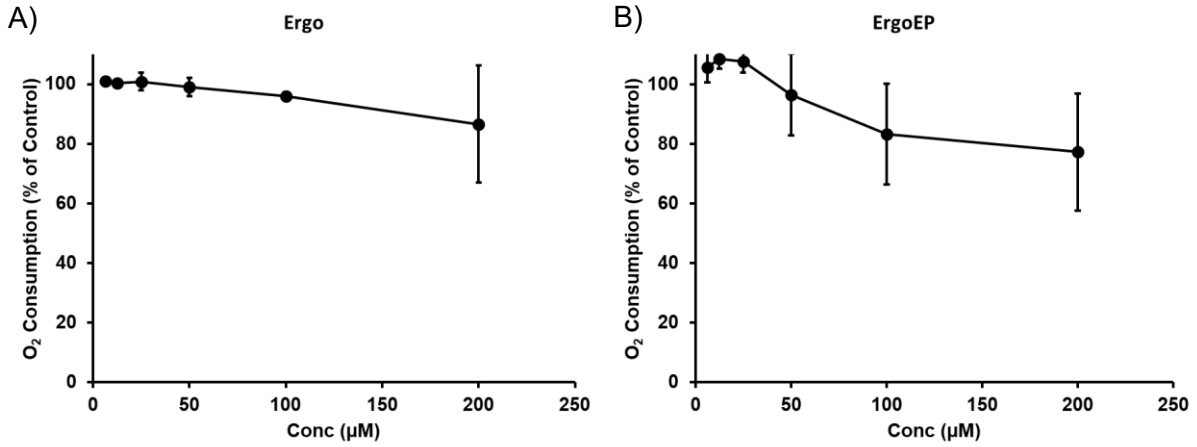

Figure 15: *Inhibition of oxygen consumption of LtP (% of control) depending on different concentrations of A) ergosterol (Ergo, 6.25 µM – 200 µM) or B) ergosterol endoperoxide (ErgoEP, 6.25 µM – 200 µM). The oxygen consumption was measured for a total of 40 minutes. The experiments were conducted in air-saturated BHI medium mixed with 140 Mio/mL LtP. Data points represent mean ± standard deviation of 4 wells.*

Likewise, DHChol and DHCholEP show only minor effects on mitochondrial oxygen consumption of LtP (Fig. 16). Effects were only observed at concentrations much higher than their IC_{50} value in LtP.

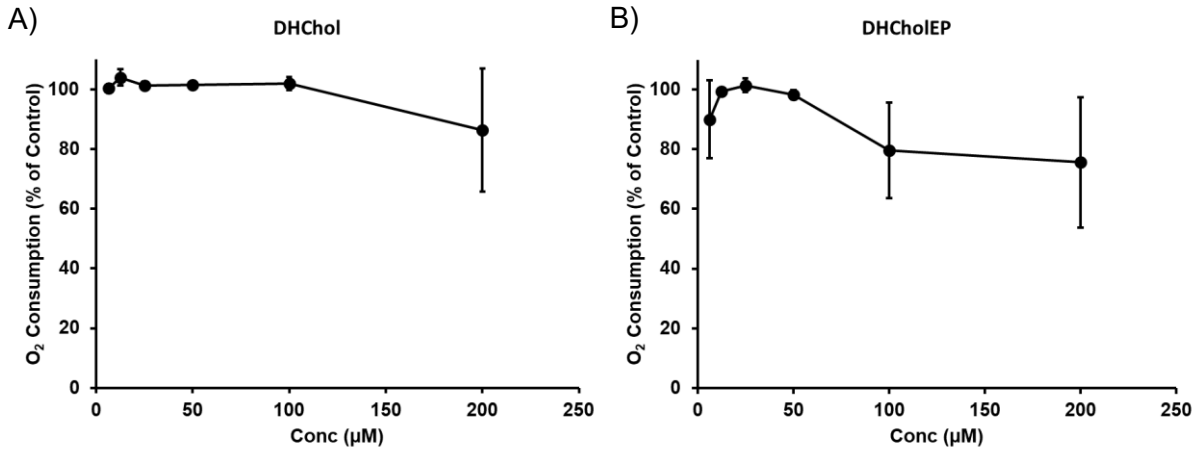

Figure 16: *Inhibition of oxygen consumption of LtP (% of control) depending on different concentrations of A) dehydrocholesterol (DHChol, 6.25 µM – 200 µM) or B) dehydrocholesterol endoperoxide (DHCholEP, 6.25 µM – 200 µM). The oxygen consumption was measured for a total of 40 minutes. The experiments were conducted in air-saturated BHI medium mixed with 140 Mio/mL LtP. Data points represent mean ± standard deviation of 4 wells.*

3.5 Influence of sterol EP on ergosterol content in LtP

The sterols and sterol EPs studied in this work have structural similarities to endogenously synthesized sterols in LtP. Therefore, it seems to be logic to study the influence of exogenous sterols and sterol EPs on endogenous sterol synthesis. Sterol synthesis in protozoa and fungi are known to be different from sterol synthesis in mammals. While in mammals Chol is a typical end product of the synthesis, in protozoa and fungi of Ergo is produced. In contrast to Chol, Ergo contains the conjugated double bond in its B-ring system, which gives rise to a significant UV absorption in the range of 252 - 320 nm. A typical example of an UV spectrum of commercial Ergo is shown in figure 17.

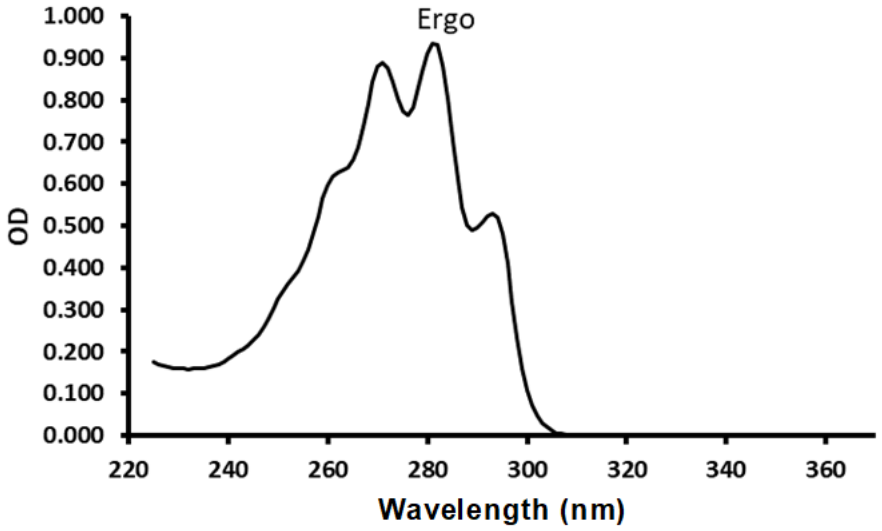

Figure 17: *Spectrum of 100 µM commercial ergosterol (Acros Organics (Geel, Belgium)) solved in ethanol, recorded between 220 nm – 360 nm wavelength. The measurement was performed in quartz glass cuvettes and 1000 µL ethanol was used as a reference. The maxima of the optical density are reached at 271 nm, 281 nm and 293 nm.*

To study the content of Ergo like sterols in LtP an analytical assay based on the saponification, liquid-liquid extraction and subsequent UV detection was established. A typical example of a spectrum of the organic extract obtained in this procedure is shown in figure 18. The spectrum shows a strong similarity to commercial Ergo.

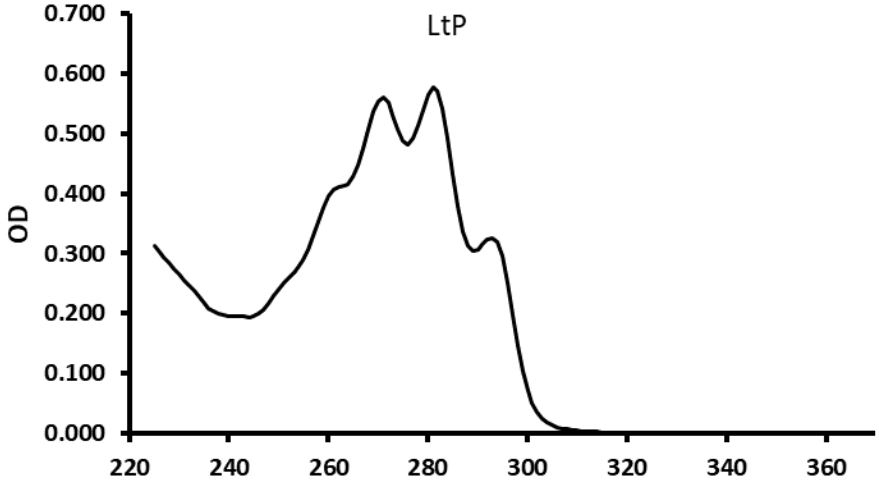

Figure 18: *Spectrum of 200 µL of hexane extract of LtP solved in ethanol, recorded between 220 nm – 360 nm wavelength. The measurement was performed in quartz glass cuvettes and 1000 µL ethanol was used as a reference. The maxima of the optical density are reached at 271 nm, 281 nm and 293 nm.*

The absorption at 281 nm was used to quantify the content of ergosterol-like sterols in LtP under different growth conditions in the presence and absence of drugs. The major difficulty of this approach was to achieve a sufficient effect of the respective compounds on the cell growth, but still having a sufficient number of cells for analysis of the Ergo-like molecule content at the end of the incubation. Therefore, LtP were cultivated in large amounts at different drug concentrations and control conditions. At the end of incubation cell pellets of LtP were isolated and subjected to the established saponification/extraction method. Obtained organic extracts were analyzed and the content of Ergo-like molecules was calculated.

Figure 19 shows a typical growth curve of LtP in the presence of different concentrations of ErgoEP in comparison to a control group containing only ethanol (Control).

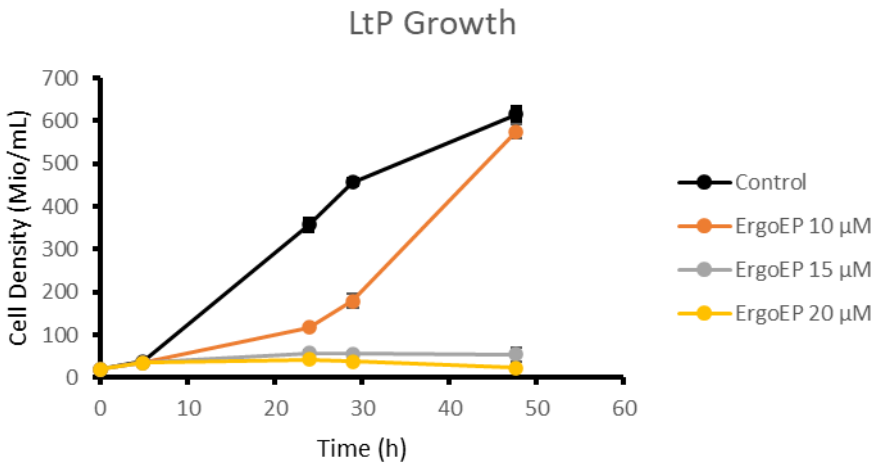

Figure 19: *Growth of LtP indicated by cell density (Mio/mL) as a function of different concentrations of ergosterol endoperoxide (ErgoEP, 10 µM – 20 µM). As control samples LtP were treated with 20 µL ethanol. The cell density was determined photometrically over a period of 48 hours. Each data point represents the mean ± standard deviation of two replicates.*

The growth behavior of LtP at fixed concentrations of ErgoEP was variable over different batch incubations of LtP. This was not overly surprising since the selected concentrations were within the range of the very steep viability-concentration curve for the respective compounds. Therefore, the correlation between the final growth percentage prior to pellet extraction and the obtained wet weight of Ergo equivalents was calculated. This correlation is shown in figure 20 for ErgoEP.

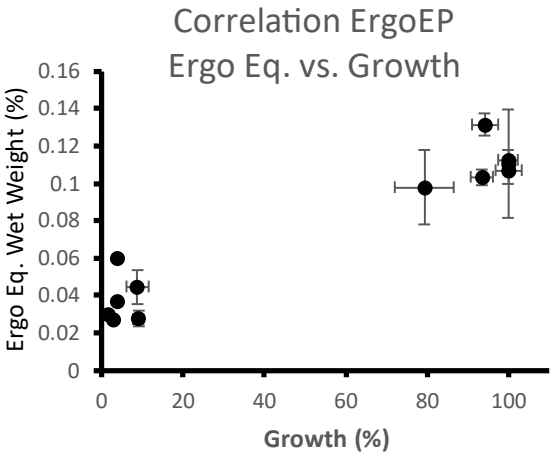

Figure 20: *Correlation of the wet weight of ergosterol equivalents (%) with growth (%) of LtP treated with ErgoEP. The LtP growth (%) was calculated relative to the maximum cell density reached by the control group. Each data point represents the mean ± standard deviation of two replicates.*

This correlation clearly demonstrated that if ErgoEP has an effect of LtP growth, it also declines the content of Ergo-like molecules in the remaining LtP cells.
Analogous experiments with different concentrations of DHCholEP were performed. Typical growth curves in the presence and absence of DHCholEP are shown in figure 21.

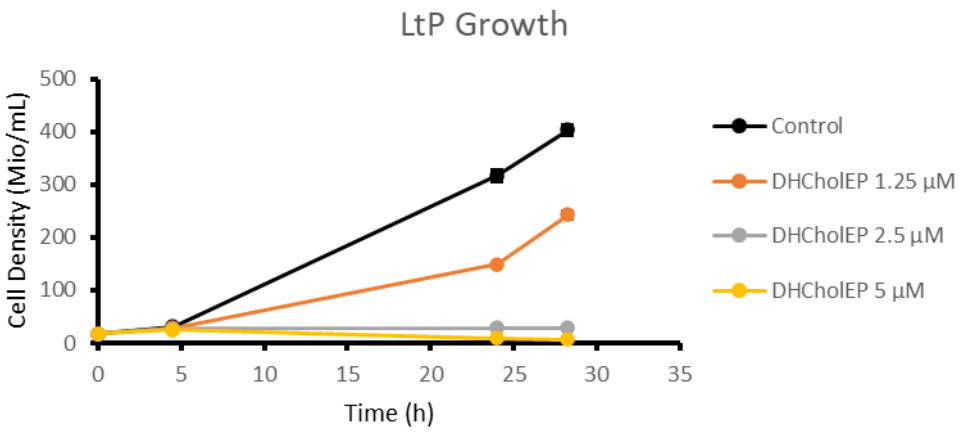

Figure 21: *Growth of LtP indicated by cell density (Mio/mL) as a function of different concentrations of dehydrocholesterol endoperoxide (DHCholEP, 1.25 µM – 5 µM). As control samples LtP were treated with 5 µL ethanol. The cell density was determined photometrically over a period of 48 hours. Each data point represents the mean ± standard deviation of two replicates.*

Again, the correlation between the content of Ergo equivalents in LtP versus their growth indicated that if DHCholEP influenced the growth of LtP under these conditions, it was also correlated with the decline of the content of Ergo-like molecules in LtP (Fig. 22).

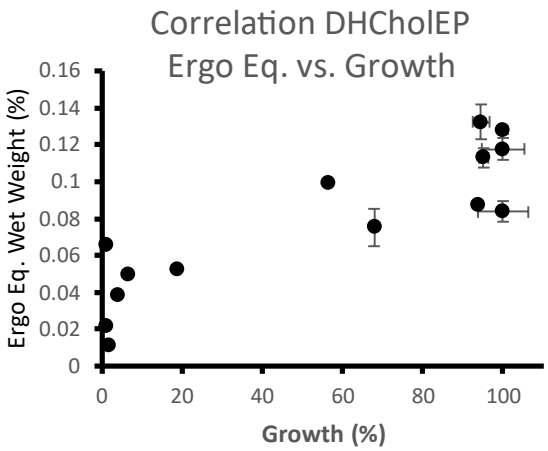

Figure 22: *Correlation of the wet weight of ergosterol equivalents (%) with growth (%) of LtP treated with dehydrocholesterol endoperoxide (DHCholEP). The LtP growth (%) was calculated relative to the maximum cell density reached by the control group. Each data point represents the mean ± standard deviation of two replicates.*

To elucidate the identity of sterols containing conjugated dienes in LtP a HPLC analysis of commercial Ergo in comparison to an untreated extract from LtP was performed and is shown in figure 23. As clearly visible the major sterol with conjugated double bonds in LtP absorbing at 281 nm is not identical to commercial Ergo.

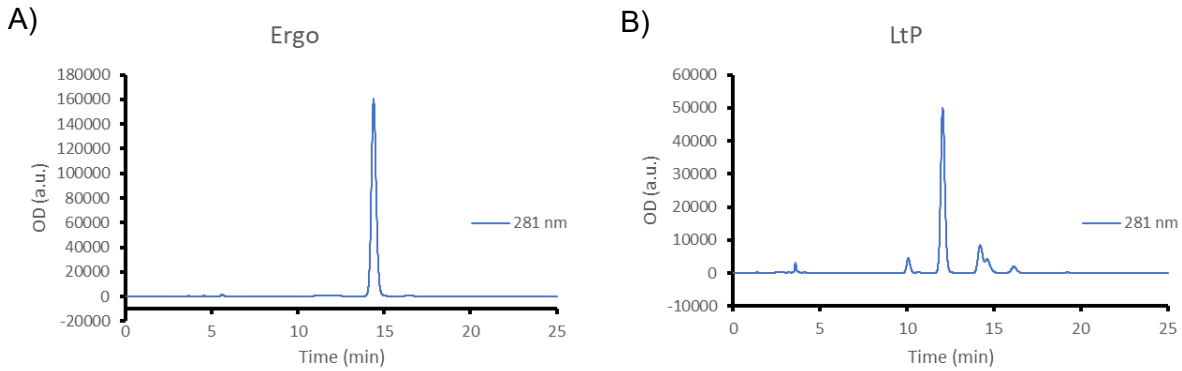

Figure 23: *HPLC chromatogram of sterols with conjugated double bonds on a RP-8 column eluted with 10 % H_2O / 90 % solvent mixture (ACN:MeOH 99:1) recorded at 281 nm. A) commercial ergosterol (Ergo) and B) solvent extract of a saponified LtP pellet.*

During HPLC analysis, spectra of the corresponding major peaks were recorded and are shown in figure 24. Comparison of the spectra shows that the major sterol in LtP with conjugated double bonds has a very similar spectrum although is not identical to Ergo.

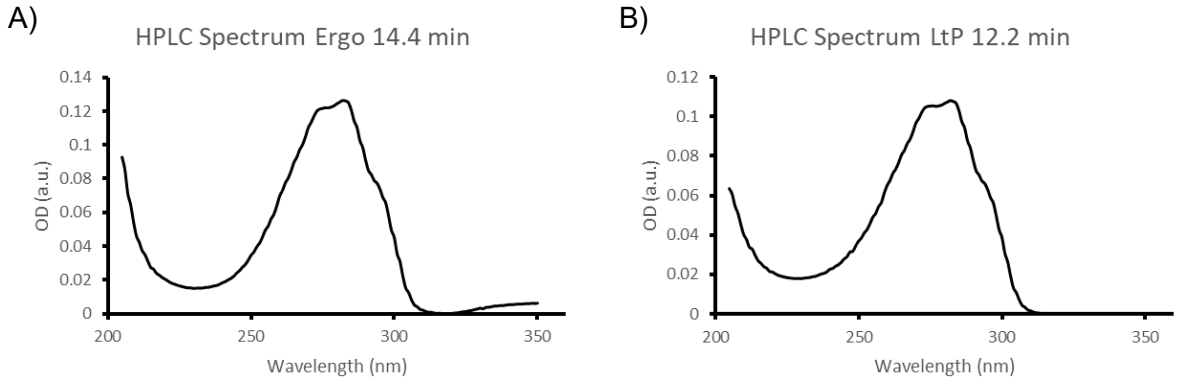

Figure 24: *UV-spectra recorded during HPLC elution at major peaks. A) spectrum of the major peak at 14.45 min of commercial ergosterol (Ergo) and B) spectrum at 12.2 min of the major peak of the LtP extract.*

4 Discussion

EPs are a diverse group of organic molecules bearing a cyclic peroxide moiety. EPs have important functions in physiology and also as defense molecules in certain organisms. EPs' activity in important physiological mechanisms are known from mammals, such as prostaglandin endoperoxide intermediates (PGH2) produced by cyclooxygenase (21). These molecules are precursors of prostaglandins, which play a vital role in the regulation of various body functions in mammals as well as in inflammation. On the other hand, plants, fungi and other microorganisms possess EPs as their defense mechanism against competing organisms (15). A typical example of this group is Asc, which is produced in *Chenopodium ambrosioides* as defense molecule (22). Likewise, artemisinin from *Artemisia annua* is a structurally different EP, which is found in its leaves and flowers (23).

A common reaction of EPs is the reductive cleavage of their peroxy group by transition metals, such as Fe^{2+}, or by homolytic cleavage (24). This explains the reactivity of EPs in cellular environments triggered by various iron-containing biomolecules (cytochromes, hemoglobin, ferritin) and low molecular iron complexes (hemin, heme, complexes with carboxylic acids and GSH) in the cell. However, the rate and specific reaction partners of different EPs can be very different, explaining the variable pharmacological effects of this compound group.

This capability of EPs has been exploited pharmacologically for the treatment of malaria using artemisinin compounds with their specific molecular properties and the specific metabolic aspects of the malaria disease (25,26). Since malaria parasites, which belong to the genus *Plansmodium*, reside in erythrocytes while *Leishmania* hide in mammalian host macrophages, the microenvironment of EPs under these conditions is very different. However, also *Leishmania* parasites acquire iron for growth inside macrophages and have importers both for heme and low molecular iron (LIT1) providing possible reaction partners for EP drugs (27,28). Upstream of these transporters, *Leishmania* even possess a *Leishmania* ferric reductase (LFR1), which continuously produces Fe^{2+} from Fe^{3+} in the extracellular space for import by LIT1 (28).

Hence, the target situations being different between Leishmania and Plasmodia, comprehensive studies on a wide range of EPs beyond artemisinin is much needed. A basic testing system for elucidation of potential antileishmanial activities of specific compounds are LtP (29). In the system of LtP so far terpene EPs, such as Asc, artemisinins and synthetic anthracene EPs have been tested (16,30,31). While structurally simple terpene EPs seem to interact with the general redox metabolism in *Leishmania*, more complex structures, such as

artemisinin and some anthracene EPs, seem to have more specific targets in *Leishmania*. Besides the natural EPs Asc and artemisinin, ErgoEP is a naturally occurring EP in many mushrooms. Several biological activities have been attributed to this EP. Since ErgoEP is structurally very different from EPs so far tested in LtP, it was highly interesting to study EPs derived from sterols in this test system.

The best-known sterol EP is ErgoEP (32). ErgoEP demonstrated various biological activities in mammalian cells, such as anticancer activities (33), suppression of inflammatory responses (34) or inhibition of lipid accumulation in adipocytes (35). Antimicrobial activities of ErgoEP were observed against *Trypanosoma* (36) and mycobacteria (37). Regarding DHCholEP even less is known. It was reported that it possesses a higher anticancer activity than ErgoEP in different cancer cell lines *in vitro* (18).

For the action or ErgoEP in mammalian cells several mechanisms were suggested: Inhibition of AKT (protein kinase B) and C-Myc (myelocytomatosis protein) (38), arrest of the cell cycle and induction of apoptosis (33). Paradoxically, even an antioxidant function of ErgoEP has been described in mushrooms (39), which is more likely to arise from Ergo itself (4).

Little is known about the antileishmanial activity and mechanism of these EPs. Therefore, in this study their effects on LtP viability, their reactivity with Fe^{2+}, the interference of NAC in antileishmanial activity, effects on mitochondrial respiration and effects on sterol synthesis in LtP were tested. Sterol synthesis in LtP is slightly different from fungi and yeasts. A simplified scheme is shown in Figure 25.

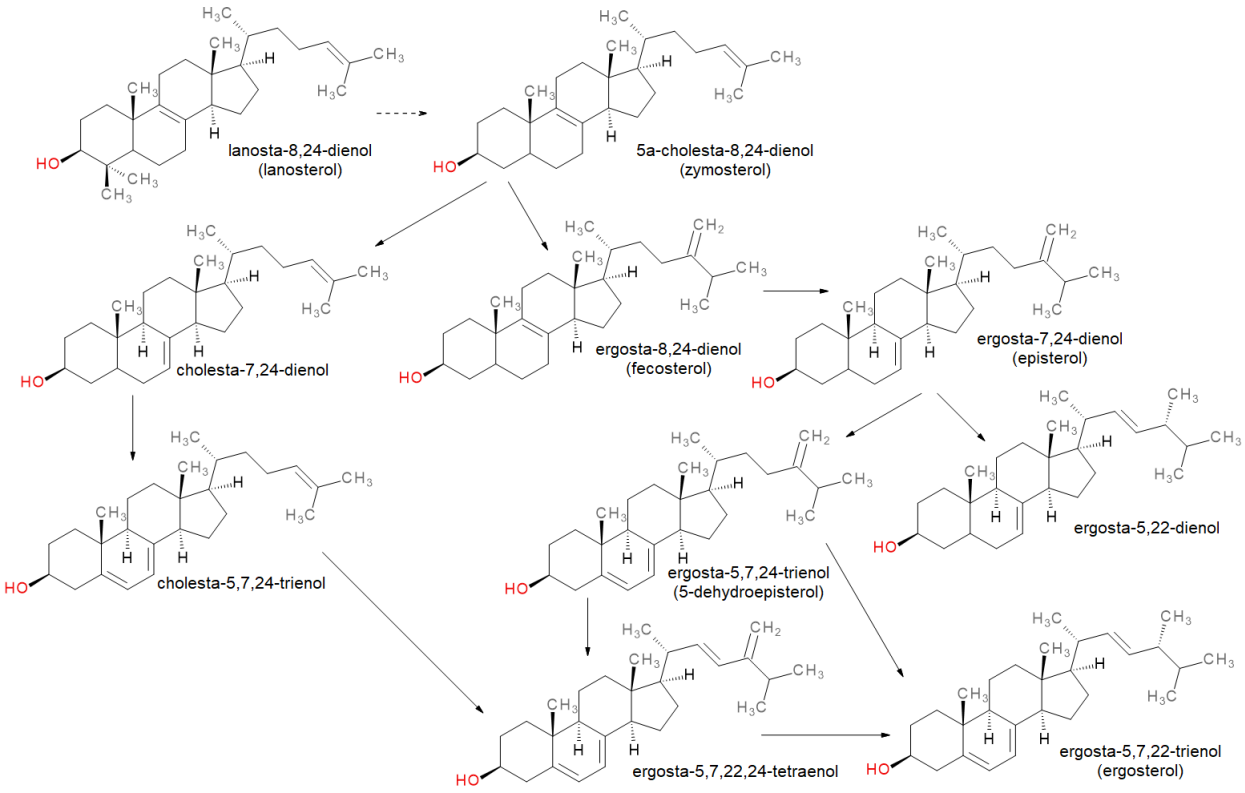

Figure 25: *Simplified scheme of ergosterol synthesis in Leishmania (40–42). Similar to ergosterol, all trienols and tetraenols shown in this scheme should exhibit a significant UV absorption around 281 nm.*

In contrast to fungi, not Ergo but the precursor 5-dehydroepisterol (5-DHE) is the most abundant sterol in *Leishmania* (42). Ergo and 5-DHE share the common element of a conjugated double bond in the B ring and, therefore, should exhibit very similar UV spectra. The synthesis of 5-DHE and Ergo from lanosterol in *Leishmania* is a multistep process involving many enzymes including 14α-demethylase (42–44), which is a target of antifungal azoles (2). Therefore, it was of interest whether ErgoEP and DHCholEP inhibit synthesis of sterols with conjugated double bonds (Ergo-like molecules: trienols and tetraenols) in LtP.

Our results showed that ErgoEP and DHCholEP inhibit LtP viability with IC_{50} values below 10 µM, and are, therefore, in a similar range as known antileishmanial compounds Pen and Mil (Fig. 6-9, Tab. 2). Even lower IC_{50} values were obtained by AmpB and the azoles KetoAz, ItraAz and MiAz in the nanomolar range. Surprisingly, sterols with conjugated double bonds in the B ring (Ergo, DHChol) also have shown antileishmanial activity in contrast to Chol lacking this structural feature. However, Ergo and DHChol were less active than their EP counterparts (Tab. 2). These activities of free (non-esterified) DHChol and Ergo are supported by observation that these are reactive sterol electrophiles which can react with proteins and amino

acids (19) while excessive endogenous sterols are often stored as ester with fatty acids in vesicels.

Considering viability-concentration curves for these compounds, it is remarkable that KetoAz and ItraAz exhibit a rather shallow curve in contrast to all other tested compounds (Fig. 9). This could be a problem in clinical application since usually dosage is set to kill all parasites, which would require much higher concentrations than expected from their IC_{50} values.

As expected, ErgoEP and DHCholEP react with Fe^{2+} forming Fe^{3+} as observed in our xylenol orange assay. Their reaction is faster than that of the terpene EP Asc and shows a non-linear time course (Fig. 11-12). Control compounds such as EtOH and Chol showed no reaction with Fe^{2+} (Fig. 10). Surprisingly, also parent sterols Ergo and DHChol reacted with Fe^{2+} quickly (Fig. 11-12, Tab. 3). This is in line with reports about their electrophile activities (19,45). Although these reactions theoretically require O_2 as reaction partner, we were not able to slow down the reaction of Ergo and DHChol with Fe^{2+} by flushing the reagents with N_2 (Tab. 4). Reasons could be the imperfectness of the experimental setup or that O_2 is not limiting for the reaction. However, we could observe that especially DHChol consumes additional O_2 during the reaction with Fe^{2+} but not Ergo (Tab. 5). This is surprising since both have conjugated double bonds in the B-ring and should have the same reactivity. A possible explanation could be that Ergo is even more lipophilic and has a lower water solubility than DHChol, which prevents a reaction with Fe^{2+} in the aqueous phase.

Since EP can produce radicals by interaction with iron in LtP which could influence viability, the prevention of this radical actions by an antioxidant should decrease the effect of the respective compound on the LtP, thus increasing its IC_{50} value. This holds true for AmpB in the presence of NAC as an antioxidant, showing a sevenfold increase of the IC_{50} value (Fig. 13). However, for azoles and Mil no effect could be observed in presence of NAC. Sterol and sterol EP actions on LtP viability were only slightly abolished by NAC. Statistically, the influence of NAC was not always significant (Tab. 6). This could have an experimental reason: NAC is highly hydrophilic while sterol EPs are highly lipophilic raising the question whether an interaction is hindered by phase separation.

Effects of antileishmanial compounds on mitochondrial O_2 consumption in LtP strongly depended on the respective compound and is generally not directly correlated with their IC_{50} values for viability. For example, AA showed significant inhibition of LtP oxygen consumption due to its specific binding to complex III in LtP mitochondria (46). In contrast, Pen did only slightly inhibit LtP oxygen consumption (Fig. 14). Sterol EPs inhibited LtP oxygen consumption only at concentrations much higher than their IC_{50} values and the effect of sterols was even

lower (Fig. 15-16).

In the last part of the study the influence of sterol EPs on the biosynthesis of Ergo-like molecules in LtP was studied. It was observed that the UV spectrum of LtP extracts shows similar absorptions as commercial Ergo (Fig. 17-18). However, HPLC measurements demonstrated: while both extracts have a similar spectrum the retention time of the major peak is different, suggesting the major sterol in LtP not to be identical with Ergo (Fig. 23-24). According to literature data the most likely candidate for this major Ergo-like sterol is 5-dehydroepisterol (5-DHE) (47). Batch incubation with ErgoEP and DHCholEP demonstrate their effect on LtP growth and that after completion of the incubation decreasing growth correlated with decreasing content of Ergo-like molecules in LtP membranes (Fig. 19-22).

So far, data demonstrated that sterol EPs have a significant antileishmanial effect in LtP and that their effect could be related to inhibition of sterol synthesis in LtP by radical attack of involved enzymes. Further studies are needed to reveal the identity of the major sterols in LtP and to corroborate the mechanism of the sterol EPs in LtP.

5 Summary

Leishmania is a genus of protozoan parasites that are transmitted to humans and animals through the bite of infected female sandflies. These parasites cause a disease called leishmaniasis. In the mammalian host the parasites are hidden from the immune system in host macrophages. This makes pharmacological treatment of leishmaniasis difficult.

Endoperoxides (EP) of natural and synthetic origin have been successfully used against malaria and in experimental models of leishmaniasis. A subgroup of EPs is derived from sterols with conjugated double bonds, such as ergosterol. So far, the influence of sterol endoperoxides on *Leishmania* viability and metabolism has not been studied in detail.

This thesis was focused on the antileishmanial activity and mechanism of the two synthetic sterol EPs: ergosterol endoperoxide (ErgoEP) and dehydrocholesterol endoperoxide (DHCholEP). For this study the model system of *Leishmania tarentolae* promastigotes (LtP) was used. The experiments were performed to verify following hypotheses: (i) sterol EPs inhibit LtP viability, (ii) their mechanism of action in LtP involves the formation of radicals by reaction with Fe^{2+}, (iii) their radical mediated damage is prevented by the radical scavenger N-acetyl cysteine (NAC), (iv) the enzymes of the Ergo synthesis pathway in Leishmania are most vulnerable due to the structure of sterol EPs which is similar to the enzymes' substrates, (v) they cause mitochondrial inhibition.

Experimentally, these ideas were addressed in chemical systems or in LtP using photometry, fluorometry and oximetry. Reactivity of EPs vs. Fe^{2+} was studied by complex formation of resulting Fe^{3+} with xylenol orange. The influence of sterol EPs and reference compounds on LtP was studied after 48 h incubation by resazurin fluorescence, yielding respective IC_{50} values. The shift of the IC_{50} values upon addition of NAC was studied to elucidate the role of radicals in their mode of action. The influence of sterol EPs on LtP respiration was evaluated in Oxoplates. After incubation of LtP with sterol EPs up to 48 h, subsequent saponification and solvent extraction, ergosterols were determined photometrically. The experiments revealed that sterol EPs react with Fe^{2+} forming Fe^{3+}, suggesting radical formation. Sterol EPs inhibited LtP viability with IC_{50} values in the low micromolar range. Their activity was marginally influenced by NAC in LtP, pointing to a minor role of radical formation. Mitochondrial inhibition by sterol EPs in LtP was observed at concentrations only far beyond their IC_{50} range. In contrast, at concentrations around their IC_{50} sterol EPs strongly inhibited Ergo synthesis. These findings provide new experimental evidence that sterol EPs target the synthesis of Ergo in *Leishmania* and, therefore, could cause significant membrane disturbance.

6 Zusammenfassung

Leishmanien sind eine Gattung protozoischer Parasiten, die durch den Stich infizierter Sandmücken auf Menschen und Tiere übertragen werden. Die Parasiten verursachen eine Krankheit namens Leishmaniose. Endoperoxide (EP) wurden in experimentellen Modellen erfolgreich gegen Leishmaniose eingesetzt. Eine Untergruppe der EP leitet sich von Sterolen mit konjugierten Doppelbindungen, z. B. Ergosterol, ab. Bislang wurde der Einfluss von Sterol-EPs auf Leishmanien noch nicht eingehend untersucht. Diese Arbeit konzentrierte sich auf die antileishmanielle Aktivität und Mechanismus der beiden Sterol-EPs: Ergosterol-Endoperoxid (ErgoEP) und Dehydrocholesterol-Endoperoxid (DHCholEP). Für diese Studie wurde das Modellsystem *Leishmania tarentolae* promastigotes (LtP) verwendet. Folgende Hypothesen wurden überprüft: (i) Sterol-EPs hemmen die Lebensfähigkeit von LtP, (ii) ihr Wirkmechanismus in LtP beinhaltet die Bildung von Radikalen durch Reaktion mit Fe^{2+}, (iii) ihre radikalvermittelte Schädigung wird durch den Radikalfänger N-Acetylcystein (NAC) verhindert, (iv) die Enzyme des Ergo-Syntheseweges in Leishmanien sind aufgrund der Struktur der Sterol-EPs, die den Substraten der Enzyme ähnlich sind, am anfälligsten. (v) sie verursachen eine mitochondriale Hemmung. Experimentell wurde die Reaktivität von EPs gegenüber Fe^{2+} wurde durch die Komplexbildung des resultierenden Fe^{3+} mit Xylenolorange untersucht. Der Einfluss von Sterol-EPs und Referenzverbindungen auf LtP wurde nach 48 h Inkubation anhand der Resazurin-Fluoreszenz untersucht, wobei die jeweiligen IC_{50}-Werte ermittelt wurden. Die Verschiebung der IC_{50}-Werte nach Zugabe von NAC wurde untersucht, um die Rolle von Radikalen in ihrer Wirkungsweise zu klären. Der Einfluss von Sterol-EPs auf die LtP-Atmung wurde in Oxoplatten untersucht. Nach bis zu 48 h Inkubation von LtP mit Sterol-EPs, anschließender Verseifung und Extraktion wurden die Ergosterole photometrisch bestimmt. Die Versuche zeigten, dass Sterol-EPs mit Fe^{2+} unter Bildung von Fe^{3+} reagieren, was auf eine Radikalbildung schließen lässt. Sterol-EPs hemmten die Lebensfähigkeit von LtP mit IC_{50}-Werten im niedrigen mikromolaren Bereich. Ihre Aktivität wurde durch NAC in LtP nur geringfügig beeinflusst, was auf eine untergeordnete Rolle der Radikalbildung hindeutet. Die mitochondriale Hemmung durch Sterol-EPs in LtP wurde nur weit jenseits ihres IC_{50}-Konzentrationsbereichs beobachtet. Im Gegensatz dazu hemmten Sterol-EPs die Ergo-Synthese bei Konzentrationen um ihren IC_{50}-Wert. Diese Ergebnisse liefern neue experimentelle Beweise dafür, dass Sterol-EPs auf die Ergo-Synthese in Leishmanien abzielen und daher erhebliche Membranstörungen verursachen könnten.

7 Abbreviations

AA	Antimycin A
AmpB	Amphotericin B
Asc	Ascaridole
BHI	Brain heart infusion
BHT	butylated hydroxytoluene
Chol	Cholesterol
DHChol	Dehydrocholesterol
DHCholEP	Dehydrocholesterol endoperoxide
DMSO	Dimethyl sulfoxide
EP	Endoperoxides
Ergo	Ergosterol
ErgoEP	Ergosterol endoperoxide
EtOH	Ethanol
IC50	Half maximal inhibitory concentration
ItraAz	Itraconazole
KetoAz	Ketoconazole
LtP	*Leishmania tarentolae* promastigotes
MeOH	Methanol
MiAz	Miconazole
Mil	Miltefosine
NAC	N-acetyl cysteine
OD	Optical density
PBS	Phosphate-buffered saline
Pen	Pentamidine
XO	Xylenol orange
Ye	Yeast extract

8 References

1. Dupont S, Lemetais G, Ferreira T, Cayot P, Gervais P, Beney L. Ergosterol biosynthesis: A fungal pathway for life on land? Evolution. 2012;66(9):2961–8.

2. Emami S, Tavangar P, Keighobadi M. An overview of azoles targeting sterol 14α-demethylase for antileishmanial therapy. Eur J Med Chem. 2017;135:241–59.

3. Vanegas JM, Contreras MF, Faller R, Longo ML. Role of unsaturated lipid and ergosterol in ethanol tolerance of model yeast biomembranes. Biophys J. 2012;102(3):507–16.

4. Dupont S, Fleurat-Lessard P, Cruz RG, Lafarge C, Grangeteau C, Yahou F, et al. Antioxidant properties of ergosterol and its role in yeast resistance to oxidation. Antioxidants(Basel). 2021;10(7):1024.

5. Jiang Q, Zhang M, Mujumdar AS. UV induced conversion during drying of ergosterol to vitamin D in various mushrooms: Effect of different drying conditions. Trends Food Sci Technol. 2020;105:200–10.

6. Bhattacharya S, Sae-Tia S, Fries BC. Candidiasis and mechanisms of antifungal resistance. Antibiotics. 2020;9(6):312.

7. Molina I, Salvador F, Sánchez-Montalvá A. The use of posaconazole against Chagas disease: Curr Opin Infect Dis. 2015;28(5):397–407.

8. Mann S, Frasca K, Scherrer S, Henao-Martinez AF, Newman S, Ramanan P, et al. A review of leishmaniasis: Current knowledge and future directions. CurrTropMedRep. 2021;8:121–32.

9. Kaye P, Scott P. Leishmaniasis: complexity at the host-pathogen interface. NatRevMicrobiol. 2011;9(8):604–15.

10. Strazzulla A, Cocuzza S, Pinzone MR, Postorino MC, Cosentino S, Serra A, et al. Mucosal leishmaniasis: An underestimated presentation of a neglected disease. BioMed Res Int. 2013;2013:1–7.

11. Olias-Molero AI, de la Fuente C, Cuquerella M, Torrado JJ, Alunda JM. Antileishmanial drug discovery and development: Time to reset the model? Microorganisms. 2021;9(12):2500.

12. Baginski M, Czub J. Amphotericin B and its new derivatives - mode of action. CurrDrug Metab. 2009;10:459–69.

13. Alonso L, Mendanha SA, Gomes RS, Dorta ML, Alonso A. Comparative EPR spectroscopy analysis of amphotericin B and miltefosine interactions with Leishmania, erythrocyte and macrophage membranes. EurJ PharmSci. 2021;163:105859.

14. Tamez-Fernández JF, Melchor-Martínez EM, Ibarra-Rivera TR, Rivas-Galindo VM. Plant-derived endoperoxides: structure, occurrence, and bioactivity. Phytochem Rev. 2020;19(4):827–64.

15. Dembitsky VM, Ermolenko E, Savidov N, Gloriozova TA, Poroikov VV. Antiprotozoal and antitumor activity of natural polycyclic endoperoxides: Origin, structures and biological activity. Molecules. 2021;26(3):686.

16. Geroldinger G, Tonner M, Fudickar W, De Sarkar S, Dighal A, Monzote L, et al. Activation of anthracene endoperoxides in Leishmania and impairment of mitochondrial functions. Molecules. 2018;23(7):1680.

17. Meza-Menchaca T, Ramos-Ligonio A, Lopez-Monteon A, Vidal LA, Kaluzhskiy LA, Shkel V, et al. Insights into ergosterol peroxide's trypanocidal activity. Biomolecules. 2019;9(9):484.

18. Tian N na, Li C, Tian N, Zhou Q xiong, Hou Y jun, Zhang B wen, et al. Syntheses of 7-dehydrocholesterol peroxides and their improved anticancer activity and selectivity over ergosterol peroxide. New J Chem. 2017;41(24):14843–6.

19. Porter NA, Xu L, Pratt DA. Reactive sterol electrophiles: Mechanisms of formation and reactions with proteins and amino acid nucleophiles. Chem Basel. 2020;2:390–417.

20. Fritsche CLE. Untersuchungen zur optimalen Kultivierung von Leishmania tarentolae. Martin-Luther-Universität Halle-Wittenberg (Germany); 2008.

21. Plastaras JP, Guengerich FP, Nebert DW, Marnett LJ. Xenobiotic-metabolizing cytochromes P450 convert prostaglandin endoperoxide to hydroxyheptadecatrienoic acid and the mutagen, malondialdehyde. J Biol Chem. 2000;275(16):11784–90.

22. Dembitsky V, Shkrob I, Hanus LO. Ascaridole and related peroxides from the genus Chenopodium. BiomedPapOlomouc. 2008;152(2):209–15.

23. Dahnum D, Abimanyu H, Senjaya A. Isolation of artemisnin as antimalarial drug from Artemisia annua L. culivated in Indonesia. Int J Basic Appl Sci. 2012;12:90–5.

24. O'Neill PM, Posner GH. A medicinal chemistry perspective on artemisinin and related endoperoxides. J Med Chem. 2004;47(12):2945–64.

25. Li Y. Qinghaosu (artemisinin): chemistry and pharmacology. Acta Pharmacol Sin. 2012 Sep;33:1141–6.

26. White NJ. Qinghaosu (Artemisinin): The price of success. Science. 2008;320(5874):330–4.

27. Huynh C, Yuan X, Miguel DC, Renberg RL, Protchenko O, Philpott CC, et al. Heme uptake by Leishmania amazonensis is mediated by the transmembrane protein LHR1. PLoS Pathog. 2012;8(7):e1002795.

28. Flannery AR, Huynh C, Mittra B, Mortara RA, Andrews NW. LFR1 ferric iron reductase of Leishmania amazonensis is essential for the generation of infective parasite forms. J Biol Chem. 2011;286(26):23266–79.

29. Taylor VM, Munoz DL, Cedeno DL, Velez ID, Jones MA, Robledo SM. Leishmania tarentolae: Utility as an in vitro model for screening of antileishmanial agents. Exp Parasitol. 2010;126(4):471–5.

30. Geroldinger G, Tonner M, Hettegger H, Bacher M, Monzote L, Walter M, et al. Mechanism of ascaridole activation in Leishmania. Biochem Pharmacol. 2017;132:48–62.

31. Geroldinger G, Tonner M, Quirgst J, Walter M, De Sarkar S, Machin L, et al. Activation of artemisinin and heme degradation in Leishmania tarentolae promastigotes: A possible link. Biochem Pharmacol. 2020;173:113737.

32. Merdivan S, Lindequist U. Ergosterol peroxide: A mushroom-derived compound with promising biological activities-A review. Int J Med Mushrooms. 2017;19:93–105.

33. He L, Shi W, Liu X, Zhao X, Zhang Z. Anticancer action and mechanism of ergosterol peroxide from Paecilomyces cicadae fermentation broth. IntJ MolSci. 2018;19(12):3935.

34. Kobori M, Yoshida M, Ohnishi-Kameyama M, Shinmoto H. Ergosterol peroxide from an edible mushroom suppresses inflammatory responses in RAW264.7 macrophages and growth of HT29 colon adenocarcinoma cells. BrJ Pharmacol. 2007;150:209–19.

35. Jeong YU, Park YJ. Ergosterol peroxide from the medicinal mushroom Ganoderma lucidum inhibits differentiation and lipid accumulation of 3T3-L1 adipocytes. Int J Mol Sci. 2020;21(2):460.

36. Ramos-Ligonio A, Lopez-Monteon A, Trigos A. Trypanocidal activity of ergosterol peroxide from Pleurotus ostreatus. PhytotherRes. 2012;26:938–43.

37. Cantrell CL, Rajab MS, Franzblau SG, Fronczek FR, Fischer NH. Antimycobacterial ergosterol-5,8-endoperoxide from Ajuga remota. Planta Med. 1999;65(8):732–4.

38. Li X, Wu Q, Bu M, Hu L, Du WW, Jiao C, et al. Ergosterol peroxide activates Foxo3-mediated cell death signaling by inhibiting AKT and c-Myc in human hepatocellular carcinoma cells. Oncotarget. 2016;7(23):33948–59.

39. Kim SW, Park SS, Min TJ, Yu KH. Antioxidant activity of ergosterol peroxide (5,8-epidioxy-5α,8α-ergosta-6,22E-dien-3β-ol) in Armillariella mellea. Bull Korean Chem Soc. 1999;20:819–23.

40. Alpizar-Sosa EA, Ithnin NRB, Wei W, Pountain AW, Weidt SK, Donachie AM, et al. Amphotericin B resistance in Leishmania mexicana: Alterations to sterol metabolism and oxidative stress response. Chatterjee M, editor. PLoS Negl Trop Dis. 2022;16(9):e0010779.

41. Yao C, Wilson ME. Dynamics of sterol synthesis during development of Leishmania spp. parasites to their virulent form. ParasitVectors. 2016;9:200.

42. Feng M, Jin Y, Yang S, Joachim AM, Ning Y, Mori-Quiroz LM, et al. Sterol profiling of Leishmania parasites using a new HPLC-tandem mass spectrometry-based method and antifungal azoles as chemical probes reveals a key intermediate sterol that supports a branched ergosterol biosynthetic pathway. Int J Parasitol Drugs Drug Resist. 2022;20:27–42.

43. McCall LI, El AA, Choi JY, Vieira DF, De MG, Johnston JB, et al. Targeting Ergosterol biosynthesis in Leishmania donovani: essentiality of sterol 14 alpha-demethylase. PLoS Negl Trop Dis. 2015;9:e0003588.

44. Bansal R, Sen SS, Muthuswami R, Madhubala R. A Plant like cytochrome P450 subfamily CYP710C1 gene in Leishmania donovani encodes sterol C-22 desaturase and its over-expression leads to resistance to amphotericin B. PLoSNeglTrop Dis. 2019;13:e0007260.

45. Wilk M, Schmitt K. Aktivierung von Steroidsystemen zu alkylierenden Agenzien. ZNaturforsch B AnorgChem OrgChem. 1981;36b:248–51.

46. Schnaufer A, Sbicego S, Blum B. Antimycin A resistance in a mutant Leishmania tarentolae strain is correlated to a point mutation in the mitochondrial apocytochrome b gene. Curr Genet. 2000;37(4):234–41.

47. Yao C, Wilson ME. Dynamics of sterol synthesis during development of Leishmania spp. parasites to their virulent form. Parasit Vectors. 2016;9(1):200.

9 List of Figures

Figure 1: Sterol biosynthesis pathways. 1

Figure 2: Chemical structures of ergosterol (Ergo) and dehydrocholesterol (DHChol). 2

Figure 3: Chemical structures of ketoconazole (KetoAz), miconazole (MiAz) and itraconazole (ItraAz). 3

Figure 4: The life cycle of Leishmania parasites. 5

Figure 5: Chemical structures of ergosterol endoperoxide (ErgoEP) and dehydrocholesterol endoperoxide (DHCholEP). 8

Figure 6: Typical example of LtP viability (%) influenced by different concentrations (0.098 µM – 200 µM) of A) ergosterol (Ergo) or B) ergosterol peroxide (ErgoEP). 17

Figure 7: Typical example of LtP viability (%) influenced by different concentrations (0.098 µM – 200 µM) of A) dehydrocholesterol (DHChol) or B) dehydrocholesterol endoperoxide (DHCholEP). 18

Figure 8: Typical example of LtP viability (%) influenced by different concentrations of A) miltefosine (Mil) (0.024 µM - 50 µM) or B) Amphotericin B (AmpB) (0.488 nM – 1000 nM). 19

Figure 9: Typical example of LtP viability (%) depending on different concentrations of A) ketoconazole (KetoAz, 0.056 nM – 10000 nM), B) miconazole (MiAz, 0.113 nM – 20000 nM) or C) itraconazole (IntraAz, 0.028 nM – 5000 nM). 19

Figure 10: XO/Fe^{3+} complex formation due to the reaction of ascaridole (Asc, 100 µM), ethanol (EtOH, 5 µL) or cholesterol (Chol, 100 µM) with Fe^{2+} (250 µM) 21

Figure 11: XO/Fe^{3+} complex formation due to the reaction of ergosterol (Ergo, 100 µM) or ergosterol endoperoxide (ErgoEP, 100 µM) with Fe^{2+} (250 µM). 21

Figure 12: XO/Fe^{3+} complex formation due to the reaction of dehydrocholesterol (DHChol, 100 µM) or dehydrocholesterol endoperoxide (DHCholEP, 100 µM) with Fe^{2+} (250 µM) 22

Figure 13: A) Typical example of LtP viability (%) depending on different concentrations (6.17 nM – 1500 nM) of amphotericin B (AmpB). 24

Figure 14: Inhibition of oxygen consumption of LtP (% of control) depending on different concentrations of A) antimycin A (AA, 1.56 nM – 50 nM) or B) pentamidine (Pen, 0.63 µM – 20 µM). 26

Figure 15: Inhibition of oxygen consumption of LtP (% of control) depending on different concentrations of A) ergosterol (Ergo, 6.25 µM – 200 µM) or B) ergosterol endoperoxide (ErgoEP, 6.25 µM – 200 µM). 27

Figure 16: Inhibition of oxygen consumption of LtP (% of control) depending on different concentrations of A) dehydrocholesterol (DHChol, 6.25 µM – 200 µM) or B) dehydrocholesterol endoperoxide (DHCholEP, 6.25 µM – 200 µM). 27

Figure 17: Spectrum of 100 µM commercial ergosterol (Acros Organics (Geel, Belgium)) solved in ethanol, recorded between 220 nm – 360 nm wavelength. 28

Figure 18: Spectrum of 200 µL of hexane extract of LtP solved in ethanol, recorded between 220 nm – 360 nm wavelength..... 29

Figure 19: Growth of LtP indicated by cell density (Mio/mL) as a function of different concentrations of ergosterol endoperoxide (ErgoEP, 10 µM – 20 µM). 30

Figure 20: Correlation of the wet weight of ergosterol equivalents (%) with growth (%) of LtP treated with ErgoEP. 30

Figure 21: Growth of LtP indicated by cell density (Mio/mL) as a function of different concentrations of dehydrocholesterol endoperoxide (DHCholEP, 1.25 µM – 5 µM). 31

Figure 22: Correlation of the wet weight of ergosterol equivalents (%) with growth (%) of LtP treated with dehydrocholesterol endoperoxide (DHCholEP). 31

Figure 23: HPLC chromatogram of sterols with conjugated double bonds on a RP-8 column eluted with 10 % H_2O / 90 % solvent mixture (ACN:MeOH 99:1) recorded at 281 nm..... 32

Figure 24: UV-spectra recorded during HPLC elution at major peaks. 32

Figure 25: Simplified scheme of ergosterol synthesis in Leishmania 35

10 List of Tables

Table 1: List of chemicals used for maintenance work and sample preparation. 10

Table 2: Influence of the respective compound on the viability of LtP. 20

Table 3: Mean XO / Fe^{3+} formation rates (nmol/min) ± standard deviation of three measurements with the respective compounds. 22

Table 4: Mean XO / Fe^{3+} formation rates (nmol/min) ± standard deviation of three measurements with the respective compounds and conditions. 23

Table 5: Mean oxygen concentration (µM) ± standard deviation of three measurements. 24

Table 6: Relative change of mean IC_{50} values (%) ± standard deviation of four replicates upon addition of N-acetyl cysteine (NAC, 2mM). 25